THE SIMPLE GOLF SIMULATOR

Cheng-Chin Chiang[1]
GTS Sporting Taiwan Co., Ltd.

Version 1.0
16 Aug, 2016

Contents

[1]mark@gtsgolf.com, chengchin.chiang@gmail.com

1 INTRODUCTION

The Physics behind the golf sport has been studied and discussed in many papers or books. Many of studies are just focused in one special topic, maybe we could not get the whole picture how much does it affect our golf performance. Also, these theories or experiments might be not easy to be understood by public. In this report I would like to re-examine and clarify some theories. I also intend to combine these theories in a calculation software, which makes them easy for us to use, evaluate and apply in the real world. The Simple Golf Simulator calculates the swing of a golf club, the launch speed of a golf ball which given by a clubhead, and the flight trajectory of a golf ball.

In this report, the swing of golf club is explained in Sec. 2, which includes the tow-rod model theory and the numerical solutions for this model. The trajectory of golf ball is discussed in Sec. 3, which includes the aerodynamic forces on a golf ball and the numerical solution for the flight trajectory. The user's guide of Simple Golf Simulator is in Sec. 4. The summary is in Sec. 5, where I list some works to be done in order to make this simulator more practical. The numerical solution I use in this simulator is Runge-Kutta method, which is an explicit iterative method and often used in temporal discretization for the approximation of solutions of differential equations. It is suitable for golf ball trajectory calculation. However, for the golf swing, since there are many parameters in the model, we have to deal with this method carefully. Three kinds of numerical solutions are listed in Sec. 2.4, if they agree with each other, then we can safely use it under such conditions.

The numerical solutions of fluid dynamics for a golf ball dimple is another big subject which is not included in this report. Usually it relies on Finite Element Method or Finite Volume Method and a huge computational work to solve the model. Some commercial or free softwares maybe can deal with it, however it still needs to be varified with the real world.

2 THE SWING OF GOLF CLUB

The dynamics of golf swing is very complex and varied with different golfers and clubs they use. Many swing parameters would affect the impact speed and direction of a clubhead on golf ball. The application of Newton's laws of motion to a simple swing model may bring some understanding of its mechanism, and we can thus search for the best way to improve the swing performance accordingly. The swing mechanism has been discussed in many papers and books. Many studies are also done and different models are proposed in order to fit the experiment results. Two-rod model with arm-club system or three-rod model with shoulder-arm-club system are majorities in these studies.

In this program we apply two-rod model (or called double pendulum model), as shown in Figure 1, to simulate the golf swing. Since the Lagrangian function of two-rod model is simple and one can easily extract arm and wrist-cock torques, which are the major parameters in swing system. The torque from shoulder joint are combined with the torque generated by golfer's trunk as an "arm torque". In two-rod model we do not need to consider the shoulder mass or moment of inertia in the swing, which are not easy to measure or define and do not directly affect the clubhead velocity. On the other hand, we take into account the bend of arm for the full-length backswing. Since the first and second moments (of inertia) of arm is changed during the swing for full-length backswing, which will be discussed in the subsection 2.2.
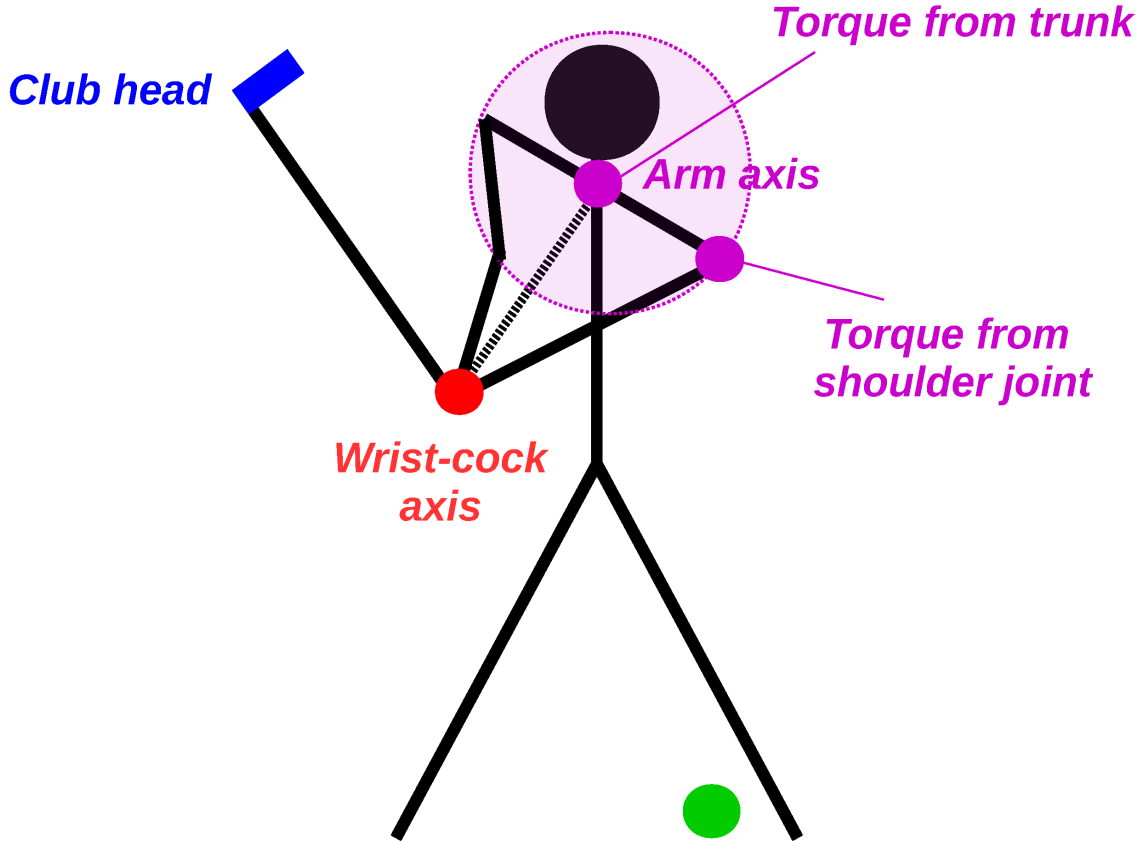

Figure 1: The two-rod model for golf swing simulation. In this model the arm torque includes the torque from trunk and the torque from shoulder joint.

2.1 Two-Rod Model

The Lagrangian function of two-rod model is described in [1] and firstly applied by Theodore P. Jorgensen [2] on the golf swing. This model can be also applied in the computer game of golf [3]. Figure 2 shows the scheme of swing plane. The angle of swing plane is defined in Figure 3. Table 3 lists the parameters of two-rod model for golf swing. We define θ as the angle through the arm has rotated clockwise from the downward direction. α represents the angle through the arm that is rotated counter-clockwise in the downswing direction. β represents the wrist-cock angle measured clockwise from the extension of the arm. The magnitude of acceleration for a golfer applies on his or her arm and club is assumed to be constant during the swing. Let the acceleration vector generated by a golfer is $\overrightarrow{a} = a_x\hat{x} - a_y\hat{y}$, as shown in Figure 2. The total acceleration in two-rod system includes the horizontal acceleration, a_x, and vertical acceleration, $g\sin\phi - a_y$, where $g\sin\phi$ is the component of gravity acceleration on a swing plane as shown in Figure 3.
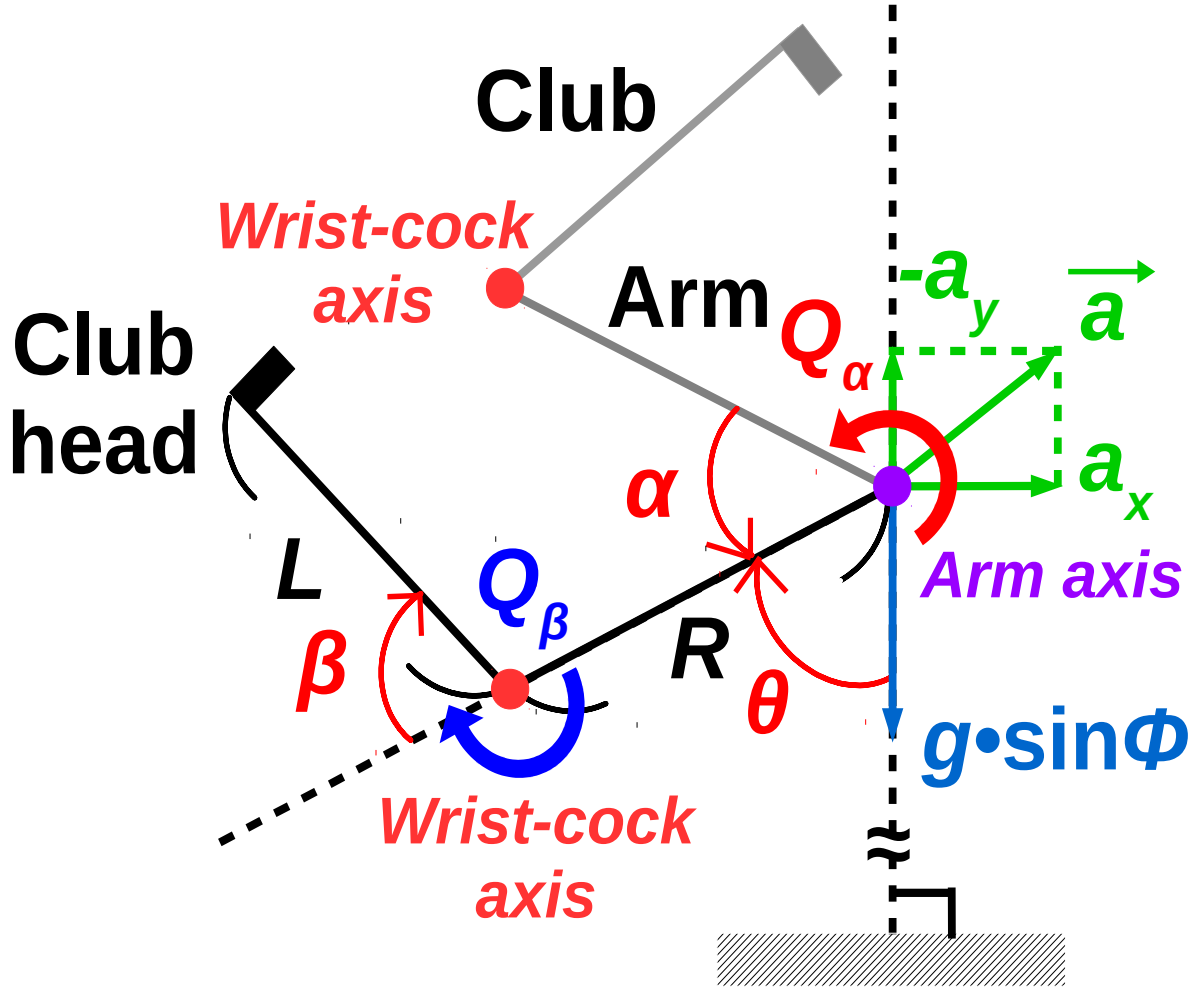

Figure 2: The scheme of the two-rod model on a golf swing plane.

The potential energy (PE) of two-rod system measured from the arm axis is

$$PE = -(S_A + M_C R)[(g\sin\phi - a_y)\cos\theta + a_x\sin\theta] \\ - S_C[(g\sin\phi - a_y)\cos(\theta + \beta) + a_x\sin(\theta + \beta)].$$
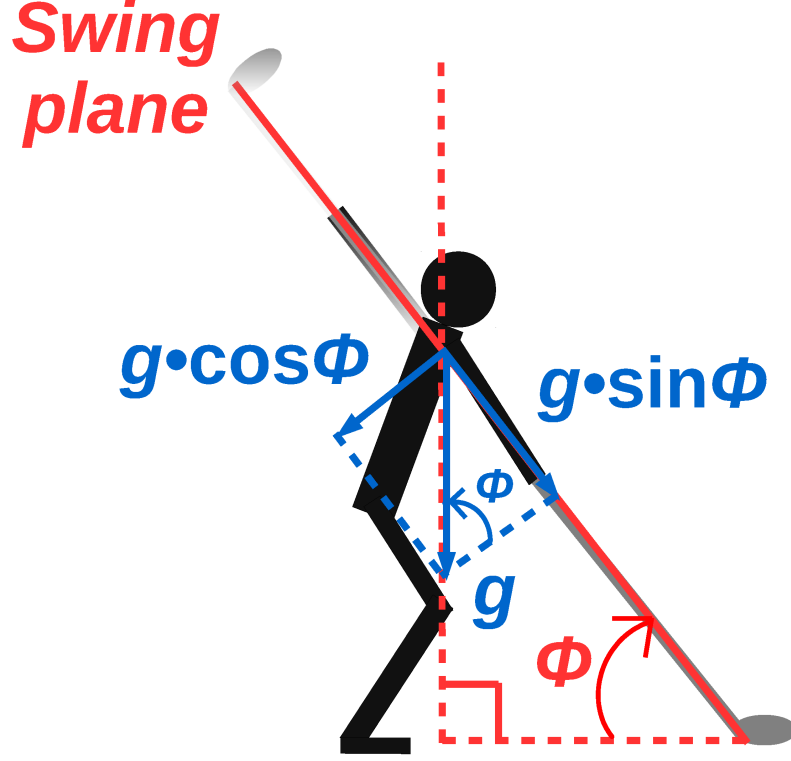
(1)

4

Figure 3: The definition of swing plane angle with respect to the magnitude of gravitational components.

The clubhead velocity is calculated as

$$V_C = \sqrt{(R^2 + L^2 + 2RL\cos\beta)\dot{\alpha}^2 + L^2\dot{\beta}^2 - 2(L^2 + RL\cos\beta)\dot{\alpha}\dot{\beta}}, \tag{2}$$

where $\dot{\alpha} = \dfrac{d\alpha}{dt}$ and $\dot{\beta} = \dfrac{d\beta}{dt}$ are angular velocities. The direction of clubhead velocity is calculated from the geometry as shown in Figure 4, where the vector of clubhead velocity $\overrightarrow{V_C}$ is the sum of two vectors $r\dot{\alpha}\hat{r}_\perp$ and $-L\dot{\beta}\hat{L}_\perp$. Let the coordinates of arm axis, wrist-cock axis and clubhead are (O_x, O_y), (w_x, w_y) and (c_x, c_y), respectively, we calculate the velocity vectors $\overrightarrow{V_C}$ as following

$$\begin{cases} \overrightarrow{r} = (c_x - O_x)\hat{x} + (c_y - O_y)\hat{y}; \\ \overrightarrow{r}_\perp = -(c_y - O_y)\hat{x} + (c_x - O_x)\hat{y}; \\ \hat{r}_\perp = \dfrac{\overrightarrow{r}_\perp}{\sqrt{(c_x - O_x)^2 + (c_y - O_y)^2}}, \end{cases}$$

$$\begin{cases} \overrightarrow{L} = (c_x - w_x)\hat{x} + (c_y - w_y)\hat{y}; \\ \overrightarrow{L}_\perp = -(c_y - w_y)\hat{x} + (c_x - w_x)\hat{y}; \\ \hat{L}_\perp = \dfrac{\overrightarrow{L}_\perp}{\sqrt{(c_x - w_x)^2 + (c_y - w_y)^2}}, \end{cases} \tag{3}$$

$$\begin{cases} r = \sqrt{R^2 + L^2 + 2RL\cos\beta}; \\ \overrightarrow{V_C} = r\dot{\alpha}\hat{r}_\perp - L\dot{\beta}\hat{L}_\perp. \end{cases}$$

Table 1: The parameters of two-rod model for golf swing.

Symbol	Meaning
R	Effective length of golfer's arm (m)
L	Club length (m)
M_C	Club mass (kg)
S_A	First moment of arm (kg-m)
S_C	First moment of club (kg-m)
J	Second moment of arm (kg-m^2)
I	Second moment of club (kg-m^2)
a_x	Horizontal acceleration by a golfer (m/sec^2)
a_y	Vertical acceleration by a golfer (m/sec^2)
g	Gravitational acceleration (9.806 m/sec^2)
θ	Arm angle measured clockwise from the downward direction (degree)
α	Downswing angle of the arm measured counter-clockwise from the start (degree)
β	Wrist-cock angle measured clockwise from the extension of arm (degree)
ϕ	Swing plane angle (degree)
V_C	clubhead velocity (m/sec)
$\theta_{\overrightarrow{V_C}}$	Angle of clubhead velocity (degree)
Q_α	Arm torque (N-m)
Q_β	Wrist-cock torque(N-m)

Let the vector of clubhead velocity $\overrightarrow{V_C} = V_{C,x}\hat{x} + V_{C,y}\hat{y}$, we can obtain the angle of clubhead velocity $\theta_{\overrightarrow{V_C}}$ by

$$\theta_{\overrightarrow{V_C}} = \sin^{-1}\left(\frac{V_{C,y}}{\sqrt{V_{C,x}^2 + V_{C,y}^2}}\right). \tag{4}$$

The clubhead velocity V_C from Eq. 2 can also be obtained by $V_C = \sqrt{V_{C,x}^2 + V_{C,y}^2}$. The angle of clubhead rotated clockwise from the downward direction is

$$\theta_C = \theta + \beta = (\theta_0 - \alpha) + \beta, \tag{5}$$

where θ_0 is the initial arm angle measured clockwise from the downward direction. Note that the variable $\theta = \theta_0 - \alpha$, so the first derivative of time of θ is

$$\frac{d\theta}{dt} = -\frac{d\alpha}{dt}, \tag{6}$$

i.e., $\dot{\theta} = -\dot{\alpha}$ or $d\theta = -d\alpha$.

The kinetic energy (KE) of two-rod system is

$$\begin{aligned}
KE &= KE(\text{Arm}) + KE(\text{Club}) \\
&= \sum_i \frac{1}{2}m_i l_i^2 \dot{\alpha}^2 + \sum_j \frac{1}{2}m_j V_j^2 \\
&= \frac{1}{2}J\dot{\alpha}^2 + \sum_j \frac{1}{2}m_j[(R^2 + l_j^2 + 2Rl_j\cos\beta)\dot{\alpha}^2 + l_j^2\dot{\beta}^2 - 2(l_j^2 + Rl_j\cos\beta)\dot{\alpha}\dot{\beta}] \\
&= \frac{1}{2}(J + I + M_C R^2 + 2RS_C\cos\beta)\dot{\alpha}^2 + \frac{1}{2}I\dot{\beta}^2 - (I + RS_C\cos\beta)\dot{\alpha}\dot{\beta}.
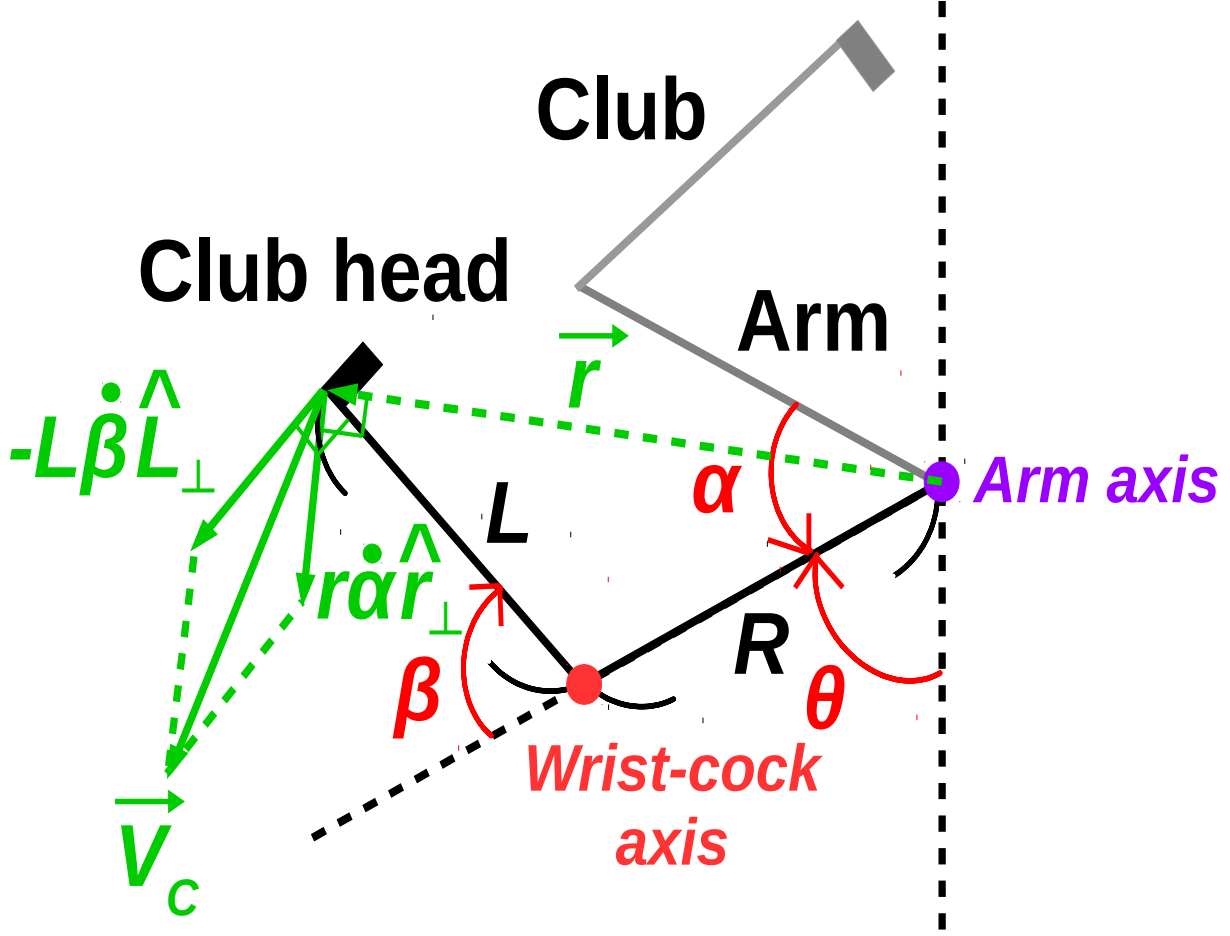\end{aligned} \tag{7}$$

Figure 4: The geometry for calculating the vector of clubhead velocity $\overrightarrow{V_C}$.

By definition, Lagrangian function is the kinetic energy subtracted by the potential energy $L = KE - PE$. We can obtain the torques of arm Q_α and wrist-cock Q_β by Lagrangian differential equations

$$\frac{d}{dt}\left(\frac{\partial L}{\partial \dot{\alpha}}\right) - \frac{\partial L}{\partial \alpha} = Q_\alpha, \qquad \frac{d}{dt}\left(\frac{\partial L}{\partial \dot{\beta}}\right) - \frac{\partial L}{\partial \beta} = Q_\beta. \tag{8}$$

The explicit forms of Q_α and Q_β are

$$\begin{aligned}
Q_\alpha = &(J + I + M_C R^2 + 2RS_C \cos\beta)\ddot{\alpha} \\
&- (I + RS_C \cos\beta)\ddot{\beta} \\
&+ (\dot{\beta}^2 - 2\dot{\alpha}\dot{\beta})RS_C \sin\beta \\
&- S_C[(g\sin\phi - a_y)\sin(\theta + \beta) - a_x\cos(\theta + \beta)] \\
&- (S_A + M_C R)[(g\sin\phi - a_y)\sin\theta - a_x\cos\theta],
\end{aligned} \tag{9}$$

$$\begin{aligned}
Q_\beta = &I\ddot{\beta} \\
&- (I + RS_C \cos\beta)\ddot{\alpha} \\
&+ \dot{\alpha}^2 RS_C \sin\beta \\
&+ S_C[(g\sin\phi - a_y)\sin(\theta + \beta) - a_x\cos(\theta + \beta)],
\end{aligned} \tag{10}$$

7

where $\ddot{\alpha} = \dfrac{d^2\alpha}{dt^2}$ and $\ddot{\beta} = \dfrac{d^2\beta}{dt^2}$ are angular accelerations. We rearrange Eq. 9 and Eq. 10 to obtain explicit forms of $\ddot{\alpha}$ and $\ddot{\beta}$:

$$
\begin{aligned}
\ddot{\alpha} = \frac{1}{(J + I + M_C R^2 + 2RS_C \cos\beta)} \Bigg[& Q_\alpha \\
& + (I + RS_C \cos\beta)\ddot{\beta} \\
& - (\dot{\beta}^2 - 2\dot{\alpha}\dot{\beta})RS_C \sin\beta \\
& + S_C[(g\sin\phi - a_y)\sin(\theta + \beta) - a_x \cos(\theta + \beta)] \\
& + (S_A + M_C R)[(g\sin\phi - a_y)\sin\theta - a_x \cos\theta] \Bigg] \\
= f_{\ddot{\alpha}}(\dot{\alpha}, \beta, \dot{\beta}, \ddot{\beta}, \theta), &
\end{aligned}
\tag{11}
$$

$$
\begin{aligned}
\ddot{\beta} = \frac{1}{I} \Bigg[& Q_\beta \\
& + (I + RS_C \cos\beta)\ddot{\alpha} \\
& - \dot{\alpha}^2 RS_C \sin\beta \\
& - S_C\left[(g\sin\phi - a_y)\sin(\theta + \beta) - a_x \cos(\theta + \beta)\right] \Bigg] \\
= f_{\ddot{\beta}}(\dot{\alpha}, \ddot{\alpha}, \beta, \theta). &
\end{aligned}
\tag{12}
$$

Note that the constant torques Q_α and Q_β result in rotational symmetries of swing tracks for wrist-cock and clubhead. On the other hand, the accelerations a_x, a_y and $g\sin\phi$ by a golfer and gravitation result in the orientation of swing tracks.

2.2 First and Second Moments of Arm

By definition, the first and second moments of arm, S_A and J, are calculated as

$$
S_A = \sum_i m_i l_i, \quad J = \sum_i m_i l_i^2
\tag{13}
$$

where m_i and l_i are the small elements of mass and rotational radius of arm from the arm axis. There are two types of backswing, restricted backswing (Type I) and full-length backwing (Type II), as shown in the Figure 5. We apply two simple arm models on two-dimensional plane, which are shown in Figure 6, to calculate the S_A and J for Type I and II backswings.

2.2.1 Type I: Restricted Backswing

As shown in the upper plot of Figure 6, the second moment of arm is calculated as

$$
\begin{aligned}
J =& 2 \int_0^{R_A/2} (R_S^2 + r_A^2 - 2R_S r_A \cos \delta) \rho_{A1} dr_A \\
&+ 2 \int_{R_A/2}^{R_A} (R_S^2 + r_A^2 - 2R_S r_A \cos \delta) \rho_{A2} dr_A \\
=& 2\rho_{A1} \left[R_S^2 r_A + \frac{r_A^3}{3} - R_S r_A^2 \cos \delta \right]\Bigg|_{r_A=0}^{r_A=R_A/2} \\
&+ 2\rho_{A2} \left[R_S^2 r_A + \frac{r_A^3}{3} - R_S r_A^2 \cos \delta \right]\Bigg|_{r_A=R_A/2}^{r_A=R_A}
\end{aligned}
\tag{14}
$$

where R_S and R_A are lengths (radii) of shoulder and arm. The densities of upper arm and forearm are $\rho_{A1} = M_{A1}/R_{A1}$ and $\rho_{A2} = M_{A2}/R_{A2}$, where M_{A1} and M_{A2} are the masses of upper arm and forearm. We have assumed the lengths of upper arm and forearm are equal, i.e., $R_{A1} = R_{A2} = R_A/2$. The angle δ and effective length of arm R are calculated by

$$
\delta = \cos^{-1}\left(\frac{R_S}{R_A} \right), \quad R = \sqrt{R_A^2 - R_S^2}.
\tag{15}
$$

The first moment of arm is calculated as

$$
\begin{aligned}
S_A =& 2 \int_0^{R_A/2} \sqrt{R_S^2 + r_A^2 - 2R_S r_A \cos \delta}\, \rho_{A1} dr_A \\
&+ 2 \int_{R_A/2}^{R_A} \sqrt{R_S^2 + r_A^2 - 2R_S r_A \cos \delta}\, \rho_{A2} dr_A \\
=& \rho_{A1} \left[R_S^2 \sin^2 \delta \sinh^{-1}\left(\frac{r_A - R_S \cos \delta}{R_S \sin \delta} \right) + (r_A - R_S \cos \delta)\sqrt{R_S^2 + r_A^2 - 2R_S r_A \cos \delta} \right]\Bigg|_{r_A=0}^{r_A=R_A/2} \\
&+ \rho_{A2} \left[R_S^2 \sin^2 \delta \sinh^{-1}\left(\frac{r_A - R_S \cos \delta}{R_S \sin \delta} \right) + (r_A - R_S \cos \delta)\sqrt{R_S^2 + r_A^2 - 2R_S r_A \cos \delta} \right]\Bigg|_{r_A=R_A/2}^{r_A=R_A},
\end{aligned}
\tag{16}
$$

for $0 < \delta \le 90°$. This integration is solved by the Maxima [4]. Note that the S_A, J and R for Type I backswing are constants during the swing.

2.2.2   Type II: Full-Length Backswing

As shown in the lower plot of Figure 6, the second moment of arm becomes

$$
\begin{aligned}
J ={}& \int_0^{R_A/2} (R_S^2 + r_A^2 - 2R_S r_A \cos \delta)\rho_{A1} dr_A \\
&+ \int_{R_A/2}^{R_A} (R_S^2 + r_A^2 - 2R_S r_A \cos \delta)\rho_{A2} dr_A \\
&+ \int_0^{R_A/2} (R_S^2 + r_A^2 - 2R_S r_A \cos \lambda)\rho_A dr_A \\
&+ \int_0^{R_A/2} (R^2 + r_A^2 - 2R r_A \cos \sigma)\rho_A dr_A \\
={}& \rho_{A1}\left[R_S^2 r_A + \frac{r_A^3}{3} - R_S r_A^2 \cos \delta \right]\Big|_{r_A=0}^{r_A=R_A/2} \\
&+ \rho_{A2}\left[R_S^2 r_A + \frac{r_A^3}{3} - R_S r_A^2 \cos \delta \right]\Big|_{r_A=R_A/2}^{r_A=R_A} \\
&+ \rho_{A1}\left[R_S^2 r_A + \frac{r_A^3}{3} - R_S r_A^2 \cos \lambda \right]\Big|_{r_A=0}^{r_A=R_A/2} \\
&+ \rho_{A2}\left[R^2 r_A + \frac{r_A^3}{3} - R r_A^2 \cos \sigma \right]\Big|_{r_A=0}^{r_A=R_A/2}
\end{aligned}
\tag{17}
$$

where the angles δ, λ and σ are calculated by the law of cosines. Given the bending angle of left arm ω, we calculated the other angles and effective length of arm as following

$$
\begin{cases}
R_A' &= R_A \sin \dfrac{\omega}{2}; \\[2mm]
\mu &= \dfrac{\pi}{2} - \dfrac{\omega}{2}; \\[2mm]
\delta &= \cos^{-1}\left(\dfrac{R_A'^2 - R_A^2 - (2R_S)^2}{-2(2R_S)R_A} \right); \\[2mm]
\lambda &= \cos^{-1}\left(\dfrac{R_A^2 - R_A'^2 - (2R_S)^2}{-2(2R_S)R_A'} \right) - \mu; \\[2mm]
R &= \sqrt{R_A^2 + R_S^2 - 2R_A R_S \cos \delta}; \\[2mm]
\epsilon &= \cos^{-1}\left(\dfrac{R_S^2 - R_A'^2 - R^2}{-2R_A' R} \right); \\[2mm]
\sigma &= \mu - \epsilon,
\end{cases}
\tag{18}
$$

The first moment of arm now becomes

$$
\begin{aligned}
S_A =& \int_0^{R_A} \sqrt{R_S^2 + r_A^2 - 2R_S r_A \cos\delta}\, \rho_A dr_A \\
&+ \int_0^{R_A/2} \sqrt{R_S^2 + r_A^2 - 2R_S r_A \cos\lambda}\, \rho_A dr_A \\
&+ \int_0^{R_A/2} \sqrt{R^2 + r_A^2 - 2R r_A \cos|\sigma|}\, \rho_A dr_A \\
=& \frac{\rho_{A1}}{2}\left[R_S^2 \sin^2\delta \sinh^{-1}\left(\frac{r_A - R_S \cos\delta}{R_S \sin\delta}\right) + (r_A - R_S \cos\delta)\sqrt{R_S^2 + r_A^2 - 2R_S r_A \cos\delta} \right]\Bigg|_{r_A=0}^{r_A=R_A/2} \\
&+ \frac{\rho_{A2}}{2}\left[R_S^2 \sin^2\delta \sinh^{-1}\left(\frac{r_A - R_S \cos\delta}{R_S \sin\delta}\right) + (r_A - R_S \cos\delta)\sqrt{R_S^2 + r_A^2 - 2R_S r_A \cos\delta} \right]\Bigg|_{r_A=R_A/2}^{r_A=R_A} \\
&+ \frac{\rho_{A1}}{2}\left[R_S^2 \sin^2\lambda \sinh^{-1}\left(\frac{r_A - R_S \cos\lambda}{R_S \sin\lambda}\right) + (r_A - R_S \cos\lambda)\sqrt{R_S^2 + r_A^2 - 2R_S r_A \cos\lambda} \right]\Bigg|_{r_A=0}^{r_A=R_A/2} \\
&+ \frac{\rho_{A2}}{2}\left[R^2 \sin^2|\sigma| \sinh^{-1}\left(\frac{r_A - R \cos|\sigma|}{R \sin|\sigma|}\right) + (r_A - R \cos|\sigma|)\sqrt{R^2 + r_A^2 - 2R r_A \cos|\sigma|} \right]\Bigg|_{r_A=0}^{r_A=R_A/2},
\end{aligned}
$$

$$(19)$$

for $0 < \{\delta, \lambda, |\sigma|\} \le 90°$. The S_A, J and R for Type II backswing are changed with the angle ω during the swing. The percentages of weights of upper arm, forearm and hand are different with each golfer. According to the statistical study, these percentages of weights for male, female and average are listed in Table 2 [5].

Table 2: The percentages of weights of upper arm, forearm and hand for male, female and average.

Segment	Males	Females	Average
Upper arm (%)	3.25	2.9	3.075
Forearm (%)	1.87	1.57	1.72
Hand (%)	0.65	0.5	0.575

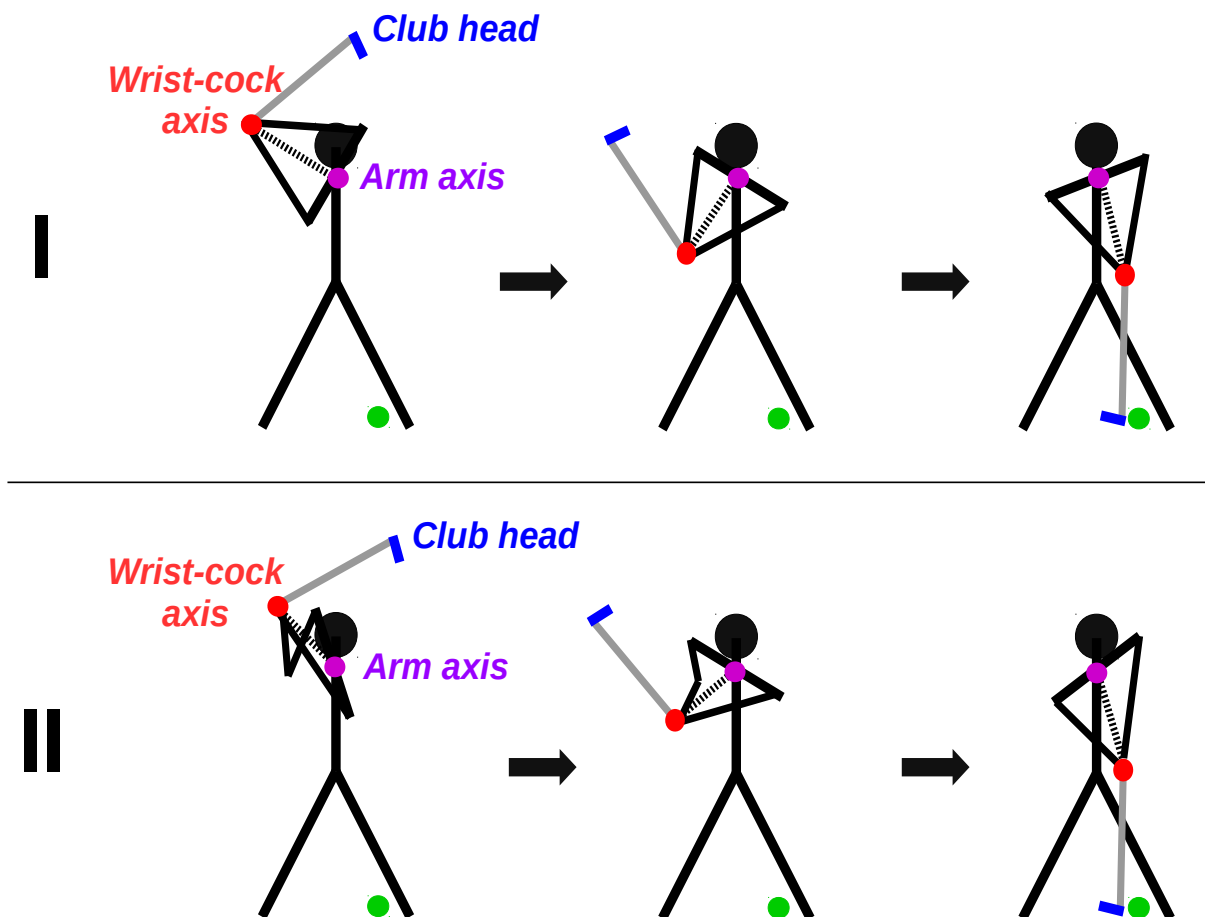Figure 5: Two types of backswing: Type I (upper) is the restricted backswing that two arms are not bent during the swing. Type II (lower) is the full-length backswing that right arm is bent at the start of swing and then gradually straight before the impact of clubhead and golf ball.
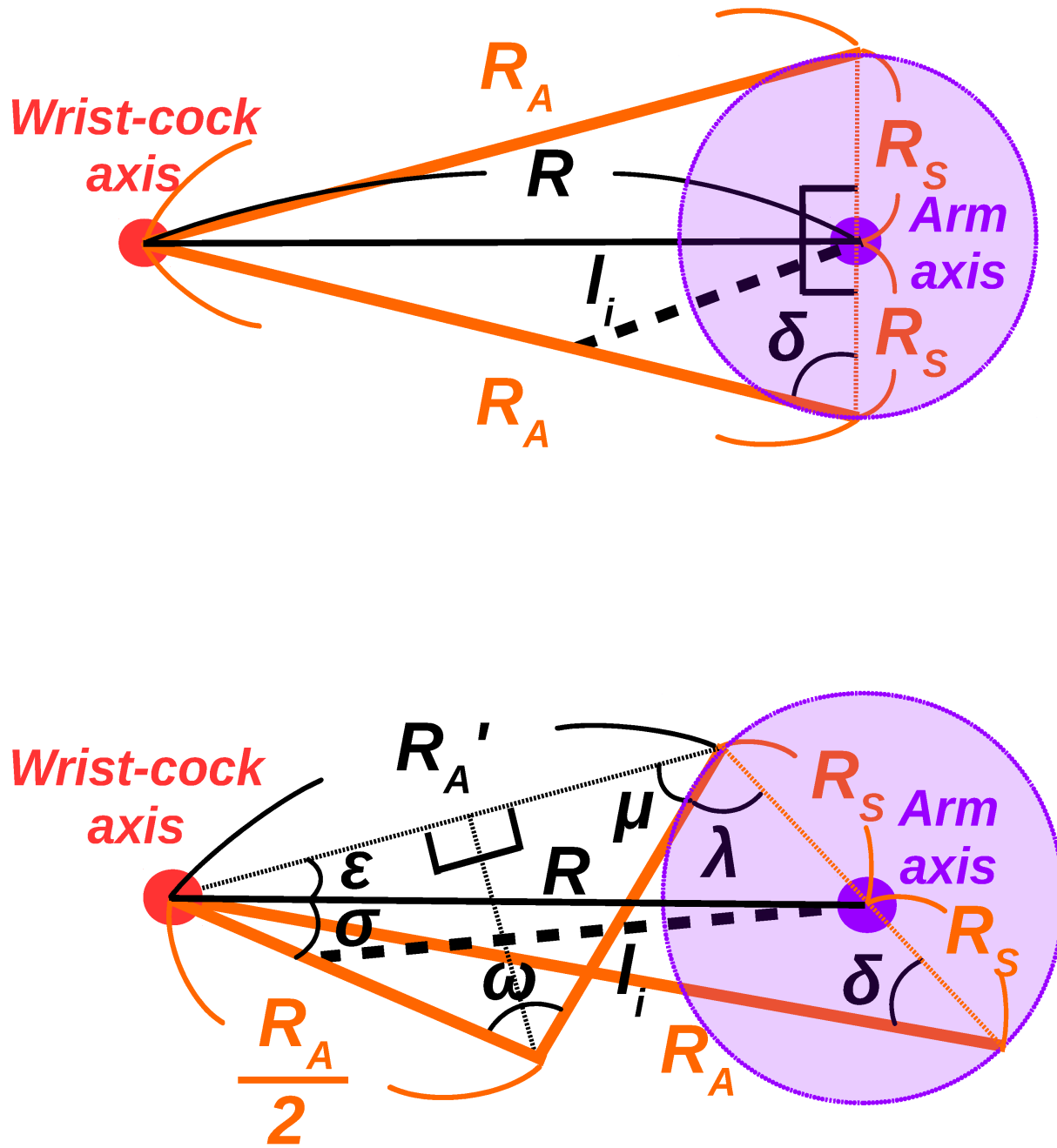
Figure 6: The geometries of arm and shoulder on 2-dimensional plane for Type I (upper) and Type II (lower) backswings.

2.3 First and Second Moments of Club

By definition, the first and second moments of club, S_C and I, are calculated as

$$S_C = \sum_j m_j l_j, \quad I = \sum_j m_j l_j^2 \tag{20}$$

where m_j and l_j are the small elements of the mass and rotational radius of club from the wrist-cock axis as shown in the upper of Figure 7. If the mass variations of club shaft and head are not large along their lengths, we can calculate S_C and I in a simple way. As shown in the lower of Figure 7, let the lengths of club shaft and head are L_{shaft} and L_{head}, the masses of club shaft and head are m_{shaft} and m_{head}, respectively. The mass centers of club shaft and head from the wrist-cock axis are $L_{\text{shaft}}/2$ and $L_{\text{shaft}} + L_{\text{head}}/2$, respectively. So the mass center of a club from wrist-cock axis L is calculated by

$$L = \frac{m_{\text{shaft}} \times L_{\text{shaft}}/2 + m_{\text{head}} \times (L_{\text{shaft}} + L_{\text{head}}/2)}{M_C}, \tag{21}$$

where $M_C = m_{\text{shaft}} + m_{\text{head}}$ is the total mass of a club. The first and second moments of a club are thus calculated by

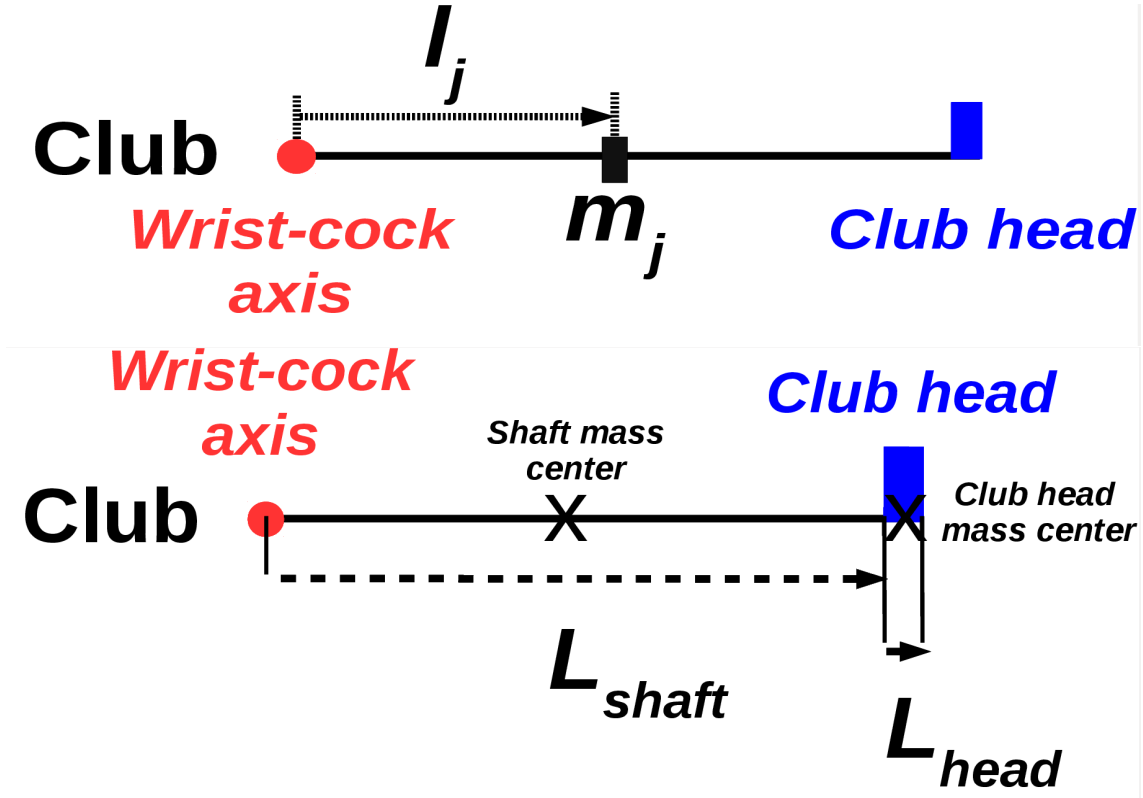$$S_A = M_C \times L, \quad I = M_C \times L^2. \tag{22}$$

Figure 7: The scheme of a golf club used to calculate the first and second moments.

2.4 Numerical Solutions of Two-Rod Model

Since Eq. 11 and Eq. 12 for solving $\ddot{\alpha}$ and $\ddot{\beta}$ are non-linear and coupled equations that there is no analytical solution. It is a typical chaos system in Physical science and we can only use numerical methods to approach the solution. Below are three ways of numerical methods to solve $\ddot{\alpha}$ and $\ddot{\beta}$.

2.4.1 Solution 1

Given the initial conditions of variables α, $\dot{\alpha}$, $\ddot{\alpha}$, β, $\dot{\beta}$, $\ddot{\beta}$ and θ, we compute the new $\ddot{\alpha}$ and $\ddot{\beta}$ by Eq. 11 and Eq. 12. For step-by-step calculations of variables changed with time, we integrate the $\ddot{\alpha}$ and $\ddot{\beta}$ with fourth-order Runge-Kutta method to obtain $\dot{\alpha}$ and $\dot{\beta}$, and then integrate $\dot{\alpha}$ and $\dot{\beta}$ with Euler method to obtain α and β. The Runge-Kutta functions $\text{RK4}_{\dot{\beta}}(\dot{\alpha}_n, \ddot{\alpha}_n, \beta_n, \dot{\beta}_n, \ddot{\beta}_n, \theta_n)$ and $\text{RK4}_{\dot{\alpha}}(\dot{\alpha}_n, \ddot{\alpha}_n, \beta_n, \dot{\beta}_n, \ddot{\beta}_n, \theta_n)$ are defined as:

$$
\begin{cases}
t_{n+1} & = t_n + h; \\
\dot{\alpha}_{n+1} & = \dot{\alpha}_n + \dfrac{h}{6}(k_1 + 2k_2 + 2k_3 + k_4) = \text{RK4}_{\dot{\alpha}}(\dot{\alpha}_n, \ddot{\alpha}_n, \beta_n, \dot{\beta}_n, \ddot{\beta}_n, \theta_n); \\
\dot{\beta}_{n+1} & = \dot{\beta}_n + \dfrac{h}{6}(q_1 + 2q_2 + 2q_3 + q_4) = \text{RK4}_{\dot{\beta}}(\dot{\alpha}_n, \ddot{\alpha}_n, \beta_n, \dot{\beta}_n, \ddot{\beta}_n, \theta_n),
\end{cases}
\tag{23}
$$

$$
\text{with}
\begin{cases}
k_1 = f_{\ddot{\alpha}}(\dot{\alpha}_n, \beta_n, \dot{\beta}_n, \ddot{\beta}_n, \theta_n); \\
k_2 = f_{\ddot{\alpha}}(\dot{\alpha}_n + \dfrac{1}{2}k_1 h, \beta_n, \dot{\beta}_n + \dfrac{1}{2}q_1 h, \ddot{\beta}_n, \theta_n); \\
k_3 = f_{\ddot{\alpha}}(\dot{\alpha}_n + \dfrac{1}{2}k_2 h, \beta_n, \dot{\beta}_n + \dfrac{1}{2}q_2 h, \ddot{\beta}_n, \theta_n); \\
k_4 = f_{\ddot{\alpha}}(\dot{\alpha}_n + k_3 h, \beta_n, \dot{\beta}_n + q_3 h, \ddot{\beta}_n, \theta_n),
\end{cases}
$$

$$
\text{and}
\begin{cases}
q_1 = f_{\ddot{\beta}}(\dot{\alpha}_n, \ddot{\alpha}_n, \beta_n, \theta_n); \\
q_2 = f_{\ddot{\beta}}(\dot{\alpha}_n + \dfrac{1}{2}k_1 h, \ddot{\alpha}_n, \beta_n, \theta_n); \\
q_3 = f_{\ddot{\beta}}(\dot{\alpha}_n + \dfrac{1}{2}k_2 h, \ddot{\alpha}_n, \beta_n, \theta_n); \\
q_4 = f_{\ddot{\beta}}(\dot{\alpha}_n + k_3 h, \ddot{\alpha}_n, \beta_n, \theta_n),
\end{cases}
\tag{24}
$$

where h is a small value of time interval (say $h = 0.0001$ sec) and $n = 0, 1, 2 \ldots N$ is the number of steps in calculations. The Euler method for integrations of $\dot{\alpha}$ and $\dot{\beta}$ are then calculated as

$$
\begin{cases}
\alpha_{n+1} & = \alpha_n + \dot{\alpha}_{n+1} h; \\
\beta_{n+1} & = \beta_n + \dot{\beta}_{n+1} h.
\end{cases}
\tag{25}
$$

The final velocity vector $\overrightarrow{V_C}$ and angle $\theta_{\overrightarrow{V_C}}$ of a clubhead can be calculated from Eq. 3 and Eq. 4 with the final step of α_N, $\dot{\alpha}_N$, β_N and $\dot{\beta}_N$. This method is reasonable while the correlation between $\ddot{\alpha}$ and $\ddot{\beta}$ is small and it will not affect the next step calculations for new $\dot{\alpha}$ and $\dot{\beta}$.

2.4.2 Solution 2

Given the initial conditions of variables α, $\dot{\alpha}$, β, $\dot{\beta}$, $\ddot{\beta}$ and θ, we compute the $\ddot{\alpha}$ from Eq. 11 and then substitute the $\ddot{\alpha}$ into Eq. 12 to compute the new $\ddot{\beta}$. In the same way, we integrate the $\ddot{\alpha}$

and $\ddot{\beta}$ step-by-step with fourth-order Runge-Kutta method. Then we integrate $\dot{\alpha}$ and $\dot{\beta}$ with Euler method to obtain α and β. The Runge-Kutta functions $\mathrm{RK4}_{\dot{\beta}}(\dot{\alpha}_n, \ddot{\alpha}_n, \beta_n, \dot{\beta}_n, \ddot{\beta}_n, \theta_n)$ and $\mathrm{RK4}_{\dot{\alpha}}(\dot{\alpha}_n, \ddot{\alpha}_n, \beta_n, \dot{\beta}_n, \ddot{\beta}_n, \theta_n)$ with $k_{1\sim4}$ and $q_{1\sim4}$ in Eq. 23 become:

$$
\begin{cases}
k_1 = f_{\ddot{\alpha}}(\dot{\alpha}_n, \beta_n, \dot{\beta}_n, \ddot{\beta}_n, \theta_n); \\[2mm]
k_2 = f_{\ddot{\alpha}}(\dot{\alpha}_n + \frac{1}{2}k_1 h, \beta_n, \dot{\beta}_n + \frac{1}{2}q_1 h, \ddot{\beta}_n(= q_1), \theta_n); \\[2mm]
k_3 = f_{\ddot{\alpha}}(\dot{\alpha}_n + \frac{1}{2}k_2 h, \beta_n, \dot{\beta}_n + \frac{1}{2}q_2 h, \ddot{\beta}_n(= q_2), \theta_n); \\[2mm]
k_4 = f_{\ddot{\alpha}}(\dot{\alpha}_n + k_3 h, \beta_n, \dot{\beta}_n + q_3 h, \ddot{\beta}_n(= q_3), \theta_n),
\end{cases}
$$
$$
\begin{cases}
q_1 = f_{\ddot{\beta}}(\dot{\alpha}_n, \ddot{\alpha}_n(= k_1), \beta_n, \theta_n); \\[2mm]
q_2 = f_{\ddot{\beta}}(\dot{\alpha}_n + \frac{1}{2}k_1 h, \ddot{\alpha}_n(= k_2), \beta_n, \theta_n); \\[2mm]
q_3 = f_{\ddot{\beta}}(\dot{\alpha}_n + \frac{1}{2}k_2 h, \ddot{\alpha}_n(= k_3), \beta_n, \theta_n); \\[2mm]
q_4 = f_{\ddot{\beta}}(\dot{\alpha}_n + k_3 h, \ddot{\alpha}_n(= k_4), \beta_n, \theta_n).
\end{cases}
\tag{26}
$$

The integrations of $\dot{\alpha}$ and $\dot{\beta}$ are then calculated by Eq. 25. This method takes the correlation between $\ddot{\alpha}$ and $\ddot{\beta}$ into account for the next step calculations of new $\dot{\alpha}$ and $\dot{\beta}$. We consider the average effects of next four and three steps of $\ddot{\alpha}$ and $\ddot{\beta}$ in integrations.

2.4.3 Solution 3

Given the initial conditions of variables α, $\dot{\alpha}$, $\ddot{\alpha}$, β, $\dot{\beta}$ and θ, we compute the $\ddot{\beta}$ from Eq. 12 and then substitute the $\ddot{\beta}$ into Eq. 11 to compute the new $\ddot{\alpha}$. In the same way, $\ddot{\alpha}$, $\ddot{\beta}$, $\dot{\alpha}$ and $\dot{\beta}$ are integrated by fourth-order Runge-Kutta and Euler methods. The Runge-Kutta functions $\mathrm{RK4}_{\dot{\beta}}(\dot{\alpha}_n, \ddot{\alpha}_n, \beta_n, \dot{\beta}_n, \ddot{\beta}_n, \theta_n)$ and $\mathrm{RK4}_{\dot{\alpha}}(\dot{\alpha}_n, \ddot{\alpha}_n, \beta_n, \dot{\beta}_n, \ddot{\beta}_n, \theta_n)$ with $k_{1\sim4}$ and $q_{1\sim4}$ in Eq. 23 now become:

$$
\begin{cases}
q_1 = f_{\ddot{\beta}}(\dot{\alpha}_n, \ddot{\alpha}_n, \beta_n, \theta_n); \\[2mm]
q_2 = f_{\ddot{\beta}}(\dot{\alpha}_n + \frac{1}{2}k_1 h, \ddot{\alpha}_n(= k_1), \beta_n, \theta_n); \\[2mm]
q_3 = f_{\ddot{\beta}}(\dot{\alpha}_n + \frac{1}{2}k_2 h, \ddot{\alpha}_n(= k_2), \beta_n, \theta_n); \\[2mm]
q_4 = f_{\ddot{\beta}}(\dot{\alpha}_n + k_3 h, \ddot{\alpha}_n(= k_3), \beta_n, \theta_n),
\end{cases}
$$
$$
\begin{cases}
k_1 = f_{\ddot{\alpha}}(\dot{\alpha}_n, \beta_n, \dot{\beta}_n, \ddot{\beta}_n(= q_1), \theta_n); \\[2mm]
k_2 = f_{\ddot{\alpha}}(\dot{\alpha}_n + \frac{1}{2}k_1 h, \beta_n, \dot{\beta}_n + \frac{1}{2}q_1 h, \ddot{\beta}_n(= q_2), \theta_n); \\[2mm]
k_3 = f_{\ddot{\alpha}}(\dot{\alpha}_n + \frac{1}{2}k_2 h, \beta_n, \dot{\beta}_n + \frac{1}{2}q_2 h, \ddot{\beta}_n(= q_3), \theta_n); \\[2mm]
k_4 = f_{\ddot{\alpha}}(\dot{\alpha}_n + k_3 h, \beta_n, \dot{\beta}_n + q_3 h, \ddot{\beta}_n(= q_4), \theta_n).
\end{cases}
\tag{27}
$$

This method takes the correlation between $\ddot{\alpha}$ and $\ddot{\beta}$ into account for the next step calculations of new $\dot{\alpha}$ and $\dot{\beta}$. We consider the average effects of next three and four steps of $\ddot{\alpha}$ and $\ddot{\beta}$ in integrations.

2.5 Simulation Studies

Here we demonstrate some simulations for golf swing. The basic settings of parameters for swing model are listed in Table 3. The torques of arm and wrist-cock with respect to time are modeled as

$$Q_\alpha(t) = Q_\alpha(1 - e^{-t/\tau_{Q\alpha}});$$

$$Q_\beta(t) = \begin{cases} 0 & \text{for } t \leq t_\theta; \\ Q_\beta(1 - e^{-(t-t_\theta)/\tau_{Q\beta}}) & \text{for } t > t_\theta, \end{cases} \tag{28}$$

where Q_α and Q_β are constants, $\tau_{Q\alpha}$ and $\tau_{Q\beta}$ are rising time of arm and wrist-cock torques, and t_θ is the starting time of wrist-cock torque while the arm angle reaches θ. In reality, the arm and wrist-cock torques could be very different with different golfers or strategies they want to apply. Six cases of simulation studies are demonstrated in the following subsections in order to let us have a basic understanding how swing performs with different parameters.

Table 3: The parameter settings of swing model.

Parameter	Value
Golfer's gender	Male
Golfer's weight (kg)	70
Golfer's shoulder radius: R_S (m)	0.17
Golfer's arm length: R_A (m)	0.6
Clubhead mass (kg)	0.2
Club shaft mass (kg)	0.1
Clubhead length (m)	0.1
Club shaft length (m)	1.0
Swing plane angle: ϕ (degree)	60
Initial arm angle: θ_0 (degree)	135
Impact arm angle: θ_f (degree)	0
Initial wrist-cock angle: β_0 (degree)	120
Impact wrist-cock angle: β_f (degree)	0
Horizontal acceleration: a_x (m/sec^2)	0
Vertical acceleration: a_y (m/sec^2)	0
Swing type	Type I
Arm torque: Q_α (N-m)	100
Rising time of arm torque: $\tau_{Q\alpha}$ (sec)	0.01
Wrist-cock torque: Q_β (N-m)	-20.64
Starting time of wrist-cock torque: t_θ	for $t_{\theta=135°}$
Rising time of wrist-cock torque: $\tau_{Q\beta}$ (sec)	0.01

2.5.1 Case 1: Compare Three Solutions of Two-Rod Model

First we compare three solutions of two-rod model as mentioned in subsection 2.4. Using the parameter settings in Table 3, we obtain the solutions of impact clubhead velocity, angle and swing time, which are shown in Table 4. The differences between these solutions are small, so we can safely apply this simulation under such parameter settings. Since this is the "Type I" swing, the first and second moments of arm are constants during the swing time. The effective length of golfer's arm is also constant, as shown in Figure 8. The simulation results are shown in Figure 9.

Table 4: Simulation results from three ways of numerical methods.

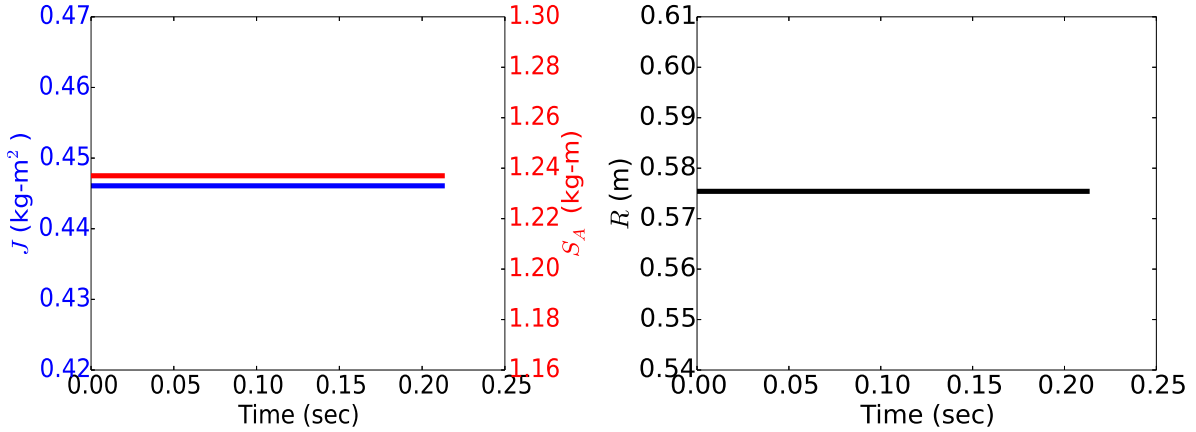|	Clubhead velocity V_C (m/sec)	Clubhead angle $\theta_{\overrightarrow{V_C}}$ (degree)	Swing time (sec)
Solution 1	52.85	0.01	0.2123
Solution 2	52.78	0.03	0.2123
Solution 3	52.80	-0.02	0.2123

Figure 8: In Type I swing, the first and second moments of arm, S_A and J, are constants during the swing time (left). The effective length of arm R is also constant (right).
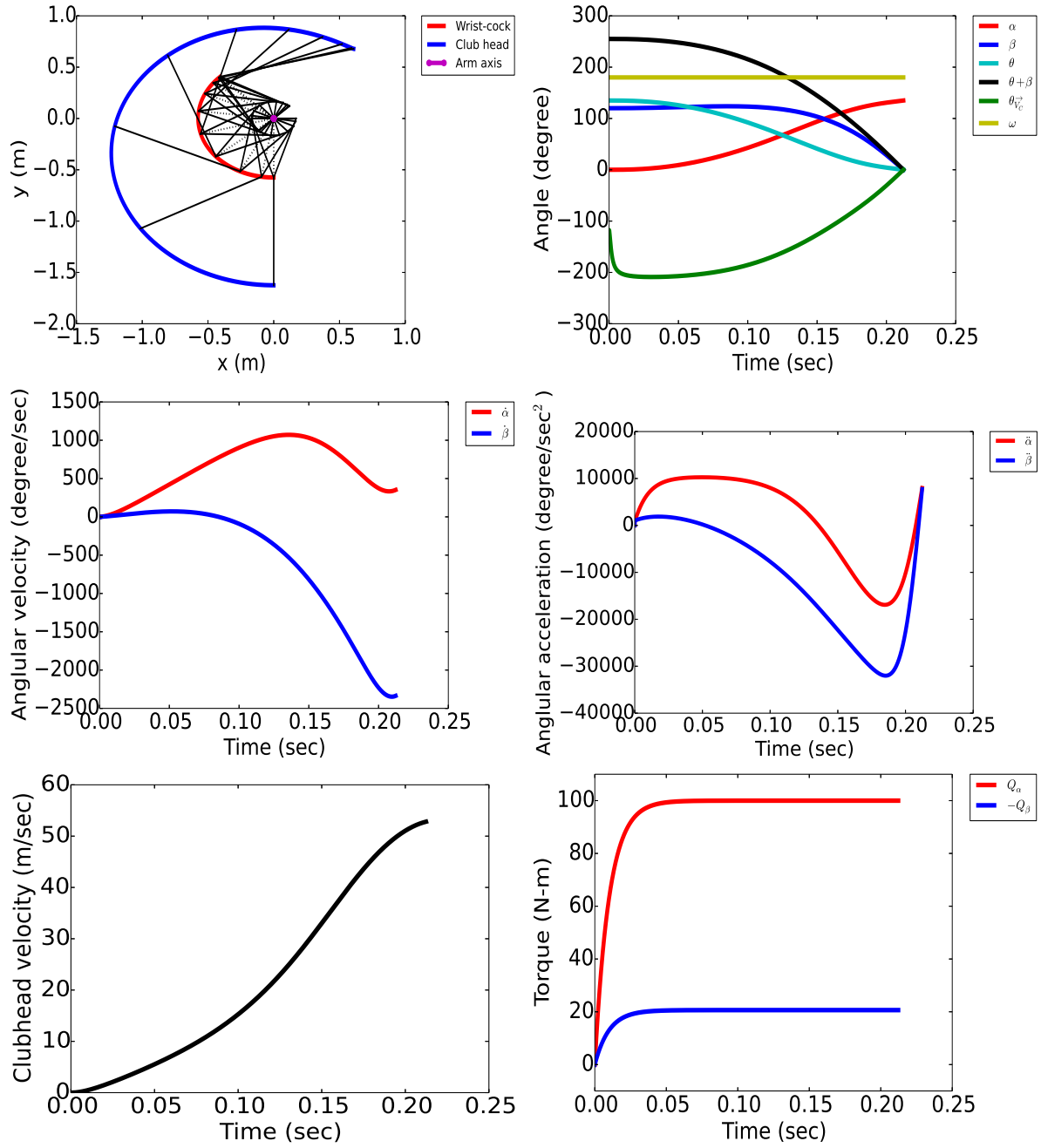
Figure 9: An example of Type I swing simulation with Solution 3. The tracks of swing for wrist-cock and clubhead (top left), the changes of angles α, β, θ, $\theta_{\overrightarrow{V_C}}$ and ω (top right), angular velocities $\dot{\alpha}$ and $\dot{\beta}$ (middle left), angular accelerations $\ddot{\alpha}$ and $\ddot{\beta}$ (middle right), clubhead velocity (bottom left), and torques Q_α and Q_β (bottom right) change with time during the swing are shown.

2.5.2 Case 2: The Effect of Arm Torque

Using the same parameter settings in Table 3, we vary the arm torque Q_α and re-optimized wrist-cock torque Q_β in order to fit the required impact angles of arm and wrist-cock, i.e., $\theta_f = 0°$ and $\beta_f = 0°$. The variations of clubhead velocity and optimized wrist-cock torque are shown in Figure 10. From simulations we find the larger of arm torque, the larger of optimized wris-cock torque in the opposite direction is needed, and the greater of clubhead velocity while impacted.
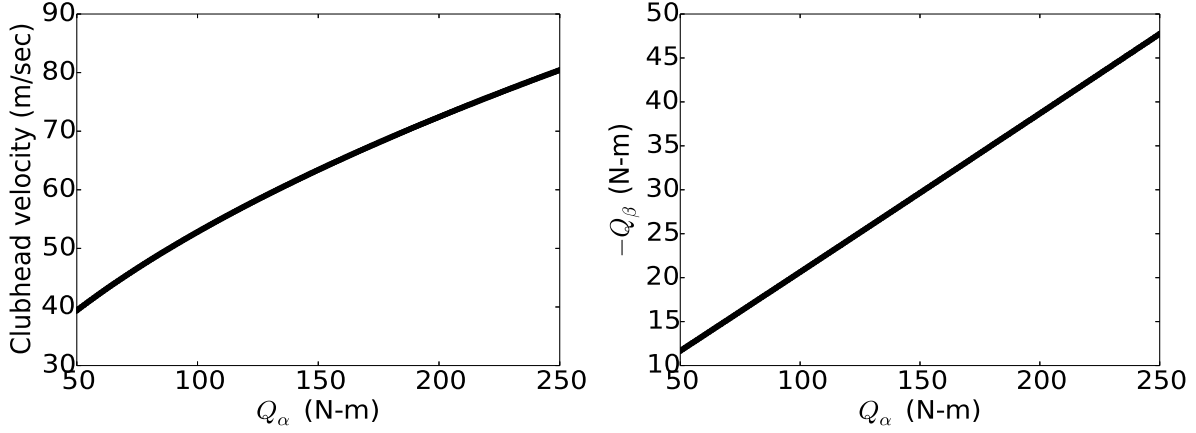

Figure 10: The clubhead velocity (left) and optimized wrist-cock torque Q_β (right) with different arm torque Q_α are shwon.

2.5.3 Case 3: The Effect of Wrist-Cock Torque

Using the same parameter settings in Table 3, now we vary the $t_{\theta=135°\sim120°}$ in Eq. 28. For $t_{\theta=135°}$, the starting time of wrist-cock torque is same with the arm torque. For $t_{\theta<135°}$, there is a delay of starting time of wrist-cock torque with respect to the arm torque. The smaller of θ from t_θ variable, the larger of time delay for wrist-cock torque with respect to the arm torque. Figure 11 shows the impact wrist-cock angle β_f for the impact arm angle $\theta_f = 0°$ vs. the wrist-cock torque Q_β setting. If we require the impact angle of wrist-cock $\beta_f = 0°$, the optimized wrist-cock torque for different t_θ setting lies on the $\beta_f = 0°$ line from Figure 11. Figure 12 shows the clubhead impact velocity and angle with respect to the wrist-cock torque Q_β for different t_θ. From simulations, we find the larger of time delay of wrist-cock torque, the larger of wris-cock torque in opposite direction is needed and the greater of clubhead impact velocity as the result.

Although the delay of starting time of wrist-cock torque can increase the clubhead impact velocity, it needs a larger wrist-cock torque in the opposite direction compared to arm torque, and it may also encounter the critical point at which the slope $\frac{d\beta}{dQ_\beta} \simeq 0$, as shown in Figure 11 for $t_{\theta<125°}$. At the critical point, the small variation of wrist-cock torque would result in the big change of clubhead impact velocity and angle. If we vary the wrist-cock torque with the optimized value ± 0.01 (N-m), the changes of resulting clubhead impact velocity and angle are defined as systematic errors. As shown in Figure 12, the systematic errors of clubhead impact velocity and angle are increased dramatically while the $t_{\theta<125°}$. So we need to avoid the critical point in reality, otherwise it may result in a big uncertainty in swing performance.

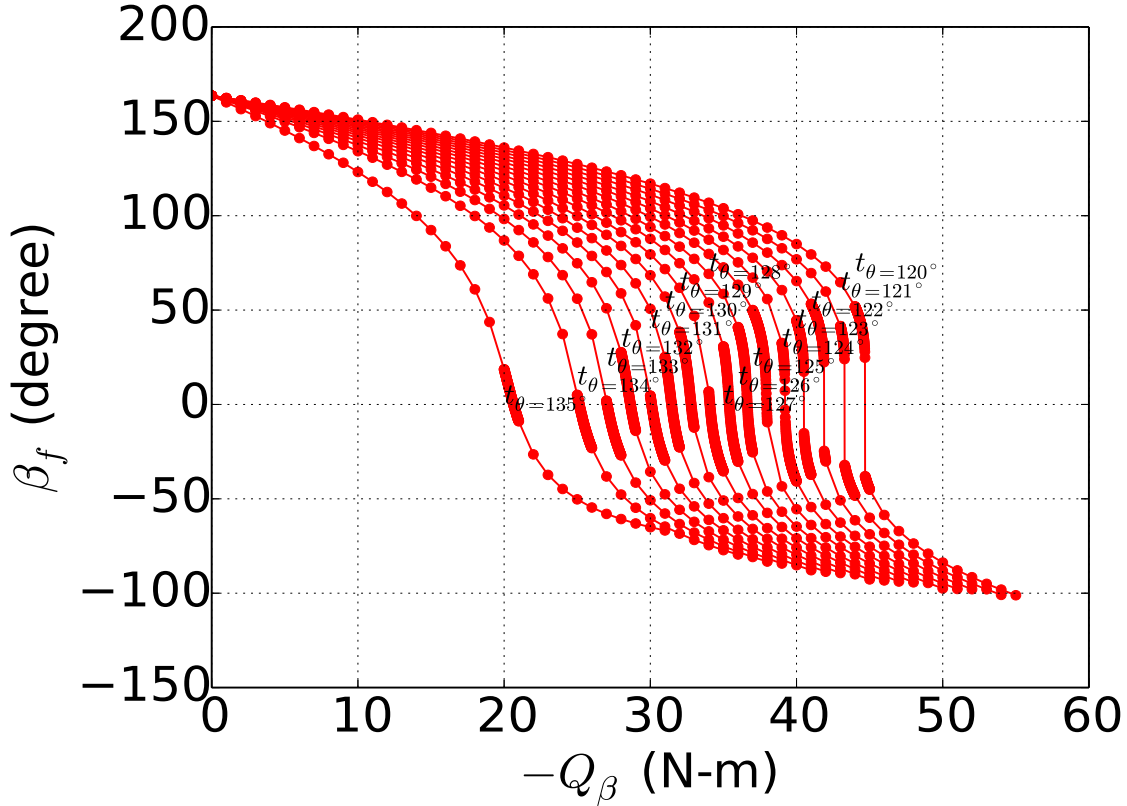Figure 11: The impact wrist-cock angle β_f for the impact arm angle $\theta_f = 0°$ vs. the wrist-cock torque Q_β setting.
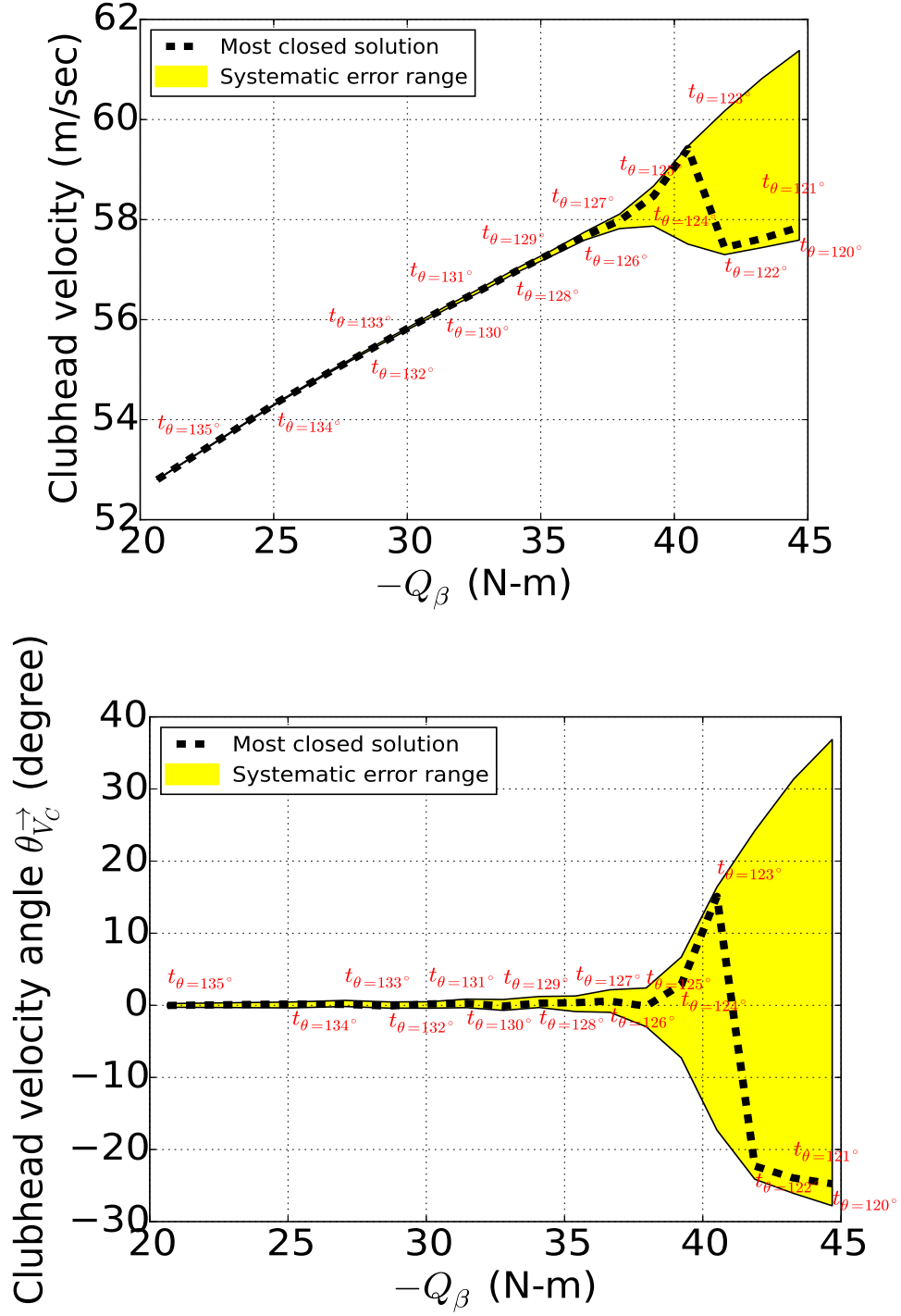
Figure 12: The clubhead impact velocity (upper) and angle (lower) with respect to the wrist-cock torque Q_β for different t_θ. The systematic errors with $Q_\beta \pm 0.01$ (N-m) are also shown.

22

2.5.4 Case 4: The Effect of Initial Arm and Wrist-cock Angles

Using the same parameter settings in Table 3, now we vary the initial arm and wrist-cock angles, θ_0 and β_0, and re-optimized the wrist-cock torque Q_β in order to fit the impact angle settings $\theta_f = 0°$ and $\beta_f = 0°$. Figure 13 shows the clubhead impact velocity and optimized wrist-cock torque for different θ_0 and β_0 settings. We find that the larger of θ_0 and β_0, the greater of clubhead impact velocity. On the other hand, the optimized wrist-cock torque $-Q_\beta$ is inverse proportional to θ_0, and with respect to β_0, there is a dip around $\beta_0 = 112°$.
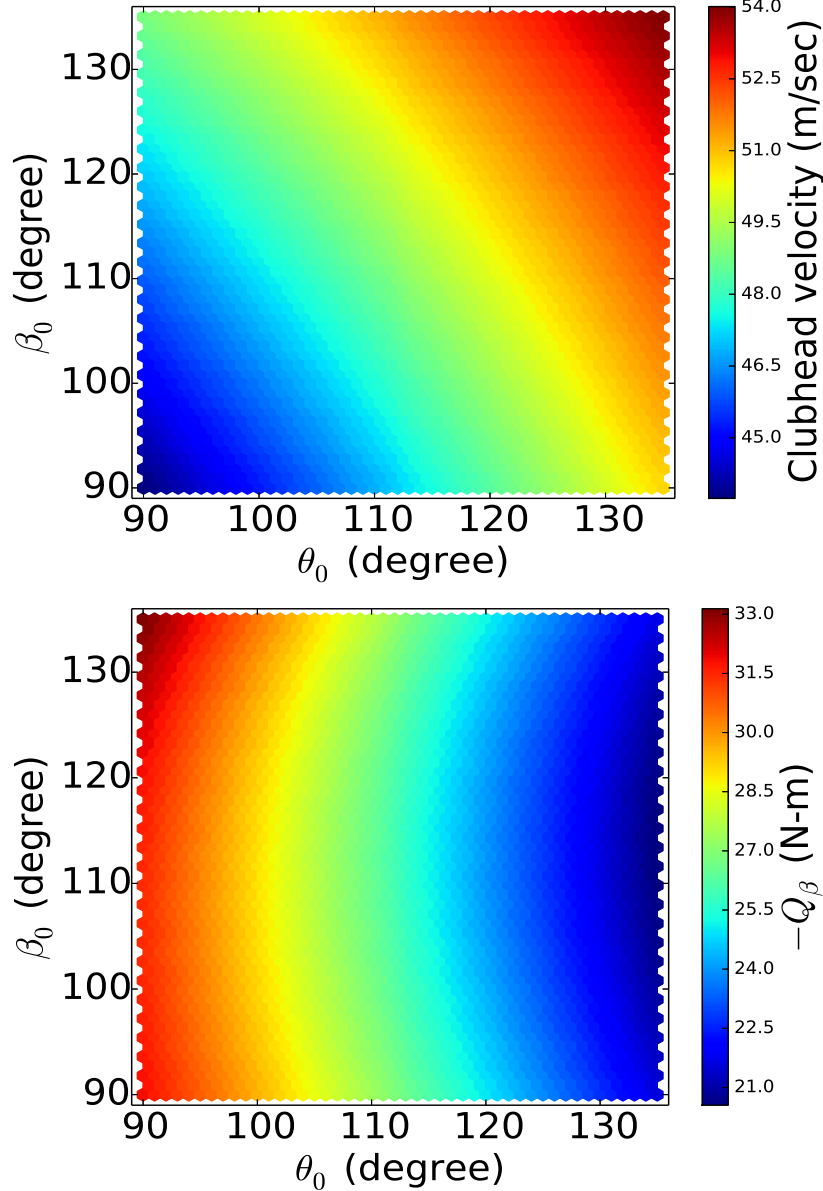

Figure 13: The clubhead impact velocity (upper) and optimized wrist-cock torque $-Q_\beta$ (lower) for different initial arm and wrist-cock angles, θ_0 and β_0.

2.5.5 Case 5: The Effect of Type I and Type II Backswings

Under the same parameter settings in Table 3, now we change the swing type from Type I to Type II. We set the minimum of left arm bending angle $\text{Min}(\omega)$ is $90°$ or for $2\sin^{-1}(1-R_S/R_A) > 90°$. The maximum of left arm bending angle $\text{Max}(\omega)$ is $180°$ before the impact of clubhead and golf ball. We also assume the evolution of left arm bending angle ω with time is proportional to α as

$$\omega(t) = \text{Min}(\omega) + \frac{\alpha(t)}{\theta_0}[\text{Max}(\omega) - \text{Min}(\omega)], \tag{29}$$

for $\alpha(t) = 0° \sim \theta_f$. In Type II swing, the effective length of arm, R, the first and second moments of arm, S_A and J, are varied with time, as shown in Figure 14. The simulation results are shown in Figure 15.
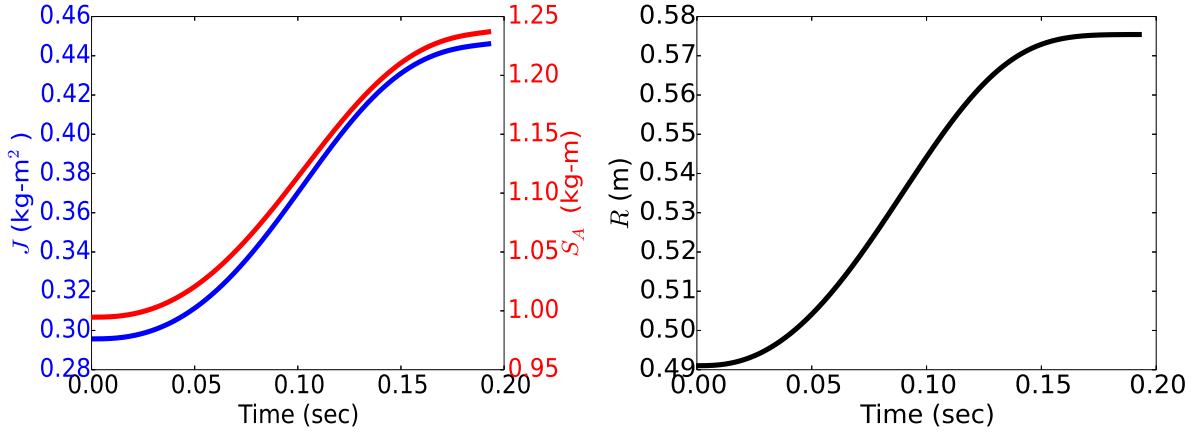

Figure 14: In Type II swing, the first and second moments of arm, S_A and J, are varied with time (left). The effective length of arm R is also varied (right).
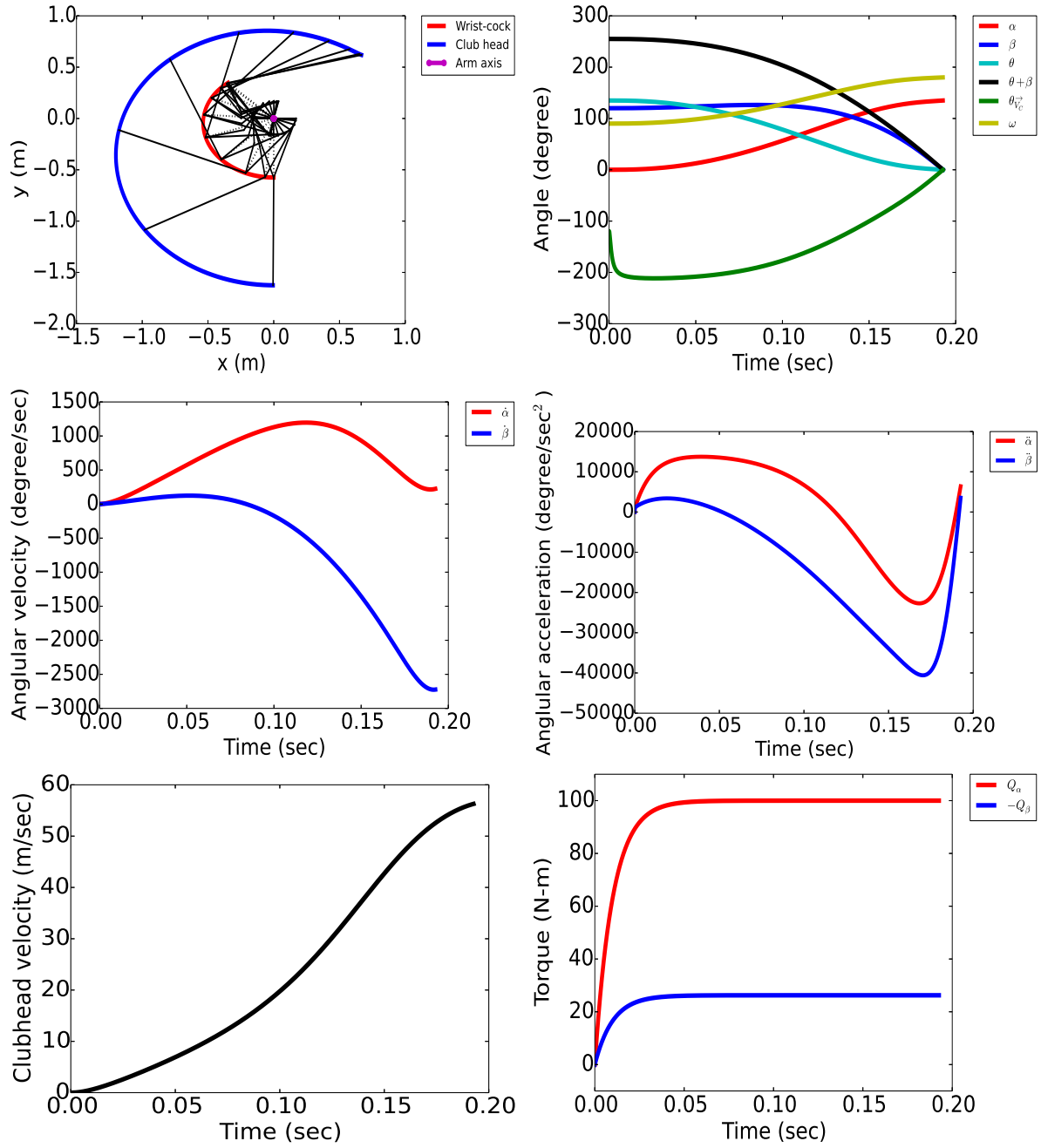
Figure 15: An example of Type II swing simulation with Solution 3. The tracks of swing for wrist-cock and clubhead (top left), the changes of angles α, β, θ, $\theta_{\overrightarrow{V_C}}$ and ω (top right), angular velocities $\dot{\alpha}$ and $\dot{\beta}$ (middle left), angular accelerations $\ddot{\alpha}$ and $\ddot{\beta}$ (middle right), clubhead velocity (bottom left), and torques Q_α and Q_β (bottom right) change with time during the swing are shown.

2.5.6   Case 6: The Effect of Clubhead Mass

By swing simulation we can calculate the impact velocity of a clubhead under various conditions. Once we know the velocity of a clubhead, the launched velocity of a golf ball can also be estimated. For the small loft associated with a club, the velocity given to a golf ball is calculated according to [6]:

$$\text{Golf ball velocity} = (1 + \text{COR}) \times \frac{M}{M + m} \times \text{Clubhead velocity}, \tag{30}$$

where M and m are the mass of clubhead and golf ball, respectively. COR is the coefficient of rebound for a golf ball. If we assume the swing arm torque $Q_\alpha = 100$ (N-m), the golf ball mass $m = 0.0458$ (kg) and COR $= 0.775$. Now we vary the clubhead mass $M = 0.05 \sim 0.3$ (kg) and re-optimized the worst-cock torque Q_β in order to fit the required impact angles, $\theta_f = 0°$ and $\beta_f = 0°$. The optimized wrist-cock torque, clubhead impact velocity and the velocity given to a golf ball from simulations are shown in Figure 16.
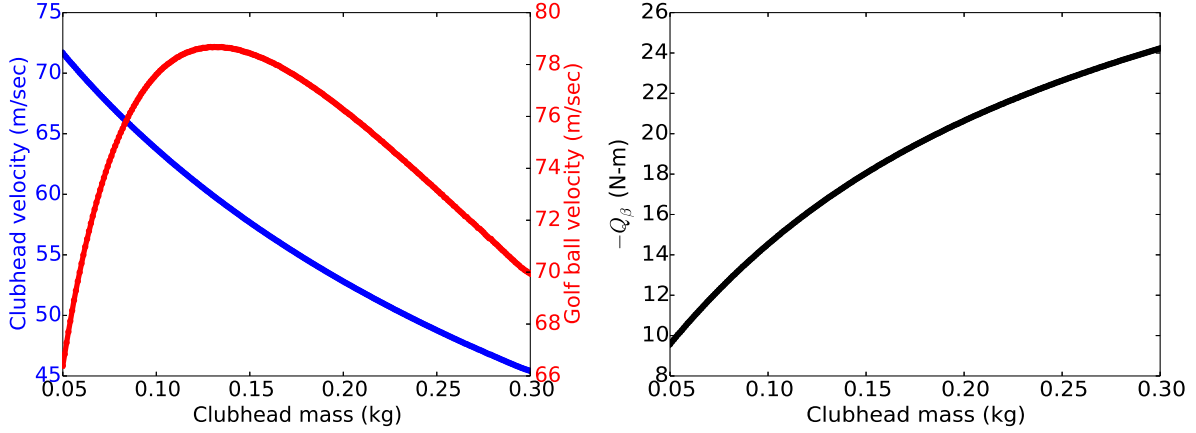

Figure 16: The clubhead impact velocity, the velocity given to a golf ball (left), and the optimized worst-cock torque Q_β (right) vs. the clubhead mass from simulations. Here we assume the swing arm torque $Q_\alpha = 100$ (N-m), the golf ball mass $m = 0.0458$ (kg) and COR $= 0.775$.

3 THE TRAJECTORY OF GOLF BALL

3.1 Aerodynamic Forces

The trajectory of golf ball is determined by its launch speed, angle, direction and aerodynamic forces. Figure 17 shows an example of streamline flow of air and aerodynamic forces on a spin and flying golf ball. The drag force F_D is caused by air friction and backward turbulence. The lift force F_L (or called Magnus force) is caused by the clockwise rotation of a ball, which is based on Bernoulli's principle. These forces are proportional to the cross-sectional area of a ball $A = \pi R^2$, air density ρ_{air} and the square of stream velocity $\overrightarrow{U}^2$:

$$
\begin{cases}
F_D = C_D \cdot A \cdot \rho_{\text{air}} \cdot \dfrac{\overrightarrow{U}^2}{2}; \\[2mm]
F_L = C_L \cdot A \cdot \rho_{\text{air}} \cdot \dfrac{\overrightarrow{U}^2}{2},
\end{cases}
\tag{31}
$$

where R is the radius of a ball. The stream velocity $\overrightarrow{U}$ is equal to the ball velocity in the opposite direction plus the wind velocity: $\overrightarrow{U} = -\overrightarrow{v}_{\text{ball}} + \overrightarrow{v}_{\text{wind}}$. C_D and C_L are the coefficients of drag and lift, respectively, and they are usually changed with the ratio of the circumferential (rotational) speed $|\overrightarrow{V}|$ of a ball to the stream speed $|\overrightarrow{U}|$. Note that $\overrightarrow{V} = \overrightarrow{w} \times \overrightarrow{R}$, where $\overrightarrow{w}$ and $\overrightarrow{R}$ are the vectors of rotational angular velocity and ball radius. So, we can represent C_D and C_L as functions of $|\overrightarrow{V}|/|\overrightarrow{U}|$, i.e., $C_D(|\overrightarrow{V}|/|\overrightarrow{U}|)$ and $C_L(|\overrightarrow{V}|/|\overrightarrow{U}|)$. The Reynolds number, Re, may be also corresponding to the drag force on a flying ball, in that case we have $C_D(Re, |\overrightarrow{V}|/|\overrightarrow{U}|)$. Re is defined as the ratio of inertial forces to viscous forces:

$$
Re = \frac{\rho_{\text{air}} \cdot |\overrightarrow{U}| \cdot D}{\mu_{\text{air}}},
\tag{32}
$$

where μ_{air} is the dynamic viscosity of air and D is the diameter of a ball, i.e., $D = 2R$. The studies of effects of $|\overrightarrow{V}|/|\overrightarrow{U}|$ and Re for C_D and C_L on flying golf balls can be found in some papers like [7, 8, 9]. A good design of dimple on golf ball can reduce the coefficient $C_D(Re, |\overrightarrow{V}|/|\overrightarrow{U}|)$, i.e., reduce the drag force and extend the flying distance. The functions $C_D(Re, |\overrightarrow{V}|/|\overrightarrow{U}|)$ and $C_L(|\overrightarrow{V}|/|\overrightarrow{U}|)$ are dependent on different kind of golf balls and they can be obtained from experimental data, as shown an example in Figure 18.
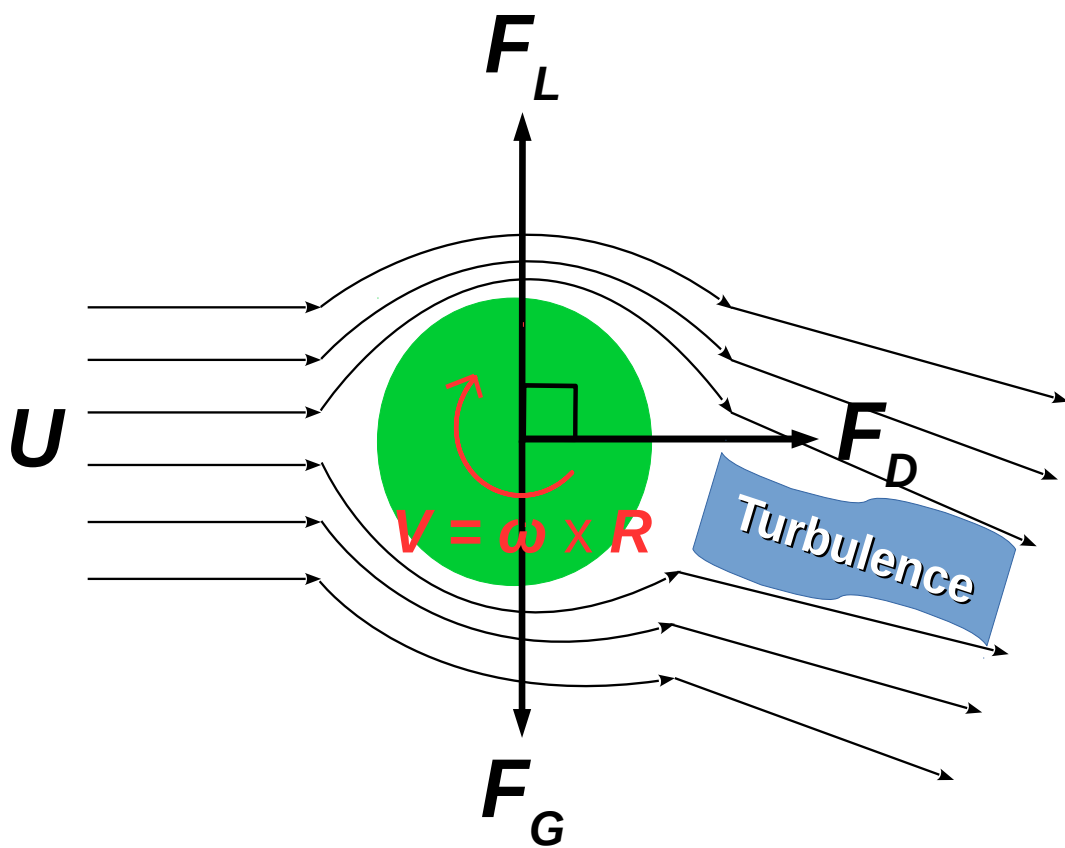
Figure 17: An example of streamline flow of air and aerodynamic forces on a spin and flying golf ball. U and V are represented as the speed of air stream and golf ball rotation. F_D, F_L and F_G are drag, lift and gravitational forces, respectively.
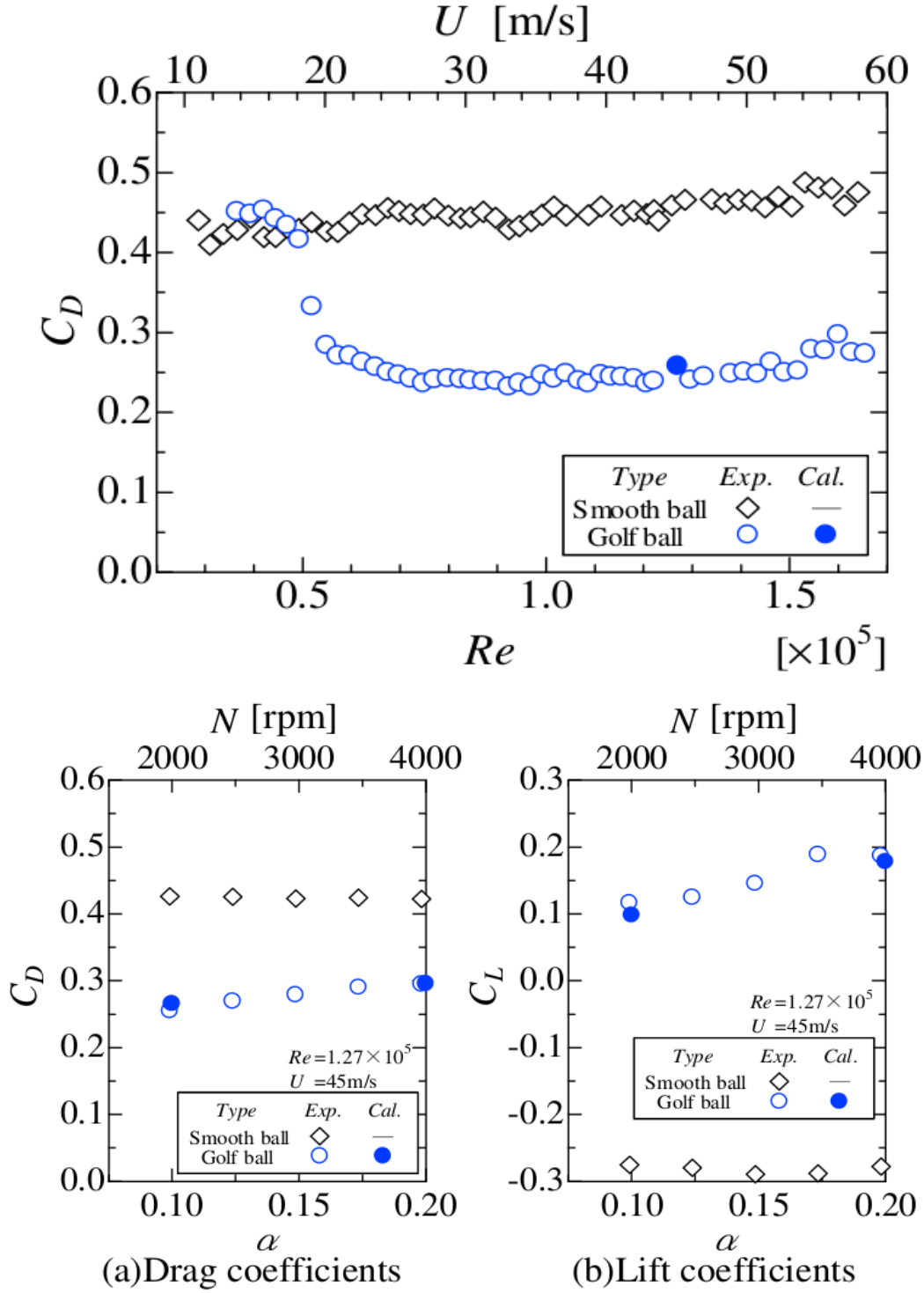
Figure 18: Adopted the figures from the paper [7]. It shows an example of experimental data for drag coefficients of golf ball without rotation (upper), drag and lift coefficient of golf ball with rotation (lower), where $\alpha = |\vec{V}|/|\vec{U}|$.

3.2 Mathematical Formula and Solution

Let the standard basis of vectors $(\hat{x}, \hat{y}, \hat{z})$, as shown in Figure 19, where $\hat{x}$ and $\hat{y}$ are orthogonal unit vectors in horizontal directions, and $\hat{z}$ is a unit vector in vertical direction. The velocity of a golf ball in three-dimension is expressed as a vector $\overrightarrow{v}_{\text{ball}} = (v_{\text{ball},x}, v_{\text{ball},y}, v_{\text{ball},z}) = v_{\text{ball},x}\hat{x} + v_{\text{ball},y}\hat{y} + v_{\text{ball},z}\hat{z}$, where

$$\begin{cases} v_{\text{ball},x} = v_{\text{ball}} \cdot \cos\theta \cdot \cos\phi; \\ v_{\text{ball},y} = v_{\text{ball}} \cdot \cos\theta \cdot \sin\phi; \\ v_{\text{ball},z} = v_{\text{ball}} \cdot \sin\theta, \end{cases} \tag{33}$$

$$\text{and} \quad v_{\text{ball}} = |\overrightarrow{v}_{\text{ball}}| = \sqrt{v_{\text{ball},x}^2 + v_{\text{ball},y}^2 + v_{\text{ball},z}^2}\,.$$

θ and ϕ are represented as elevation and direction angles for a ball. So the unit vector of ball velocity is

$$\frac{\overrightarrow{v}_{\text{ball}}}{|\overrightarrow{v}_{\text{ball}}|} = \cos\theta\cos\phi\,\hat{x} + \cos\theta\sin\phi\,\hat{y} + \sin\theta\,\hat{z}. \tag{34}$$
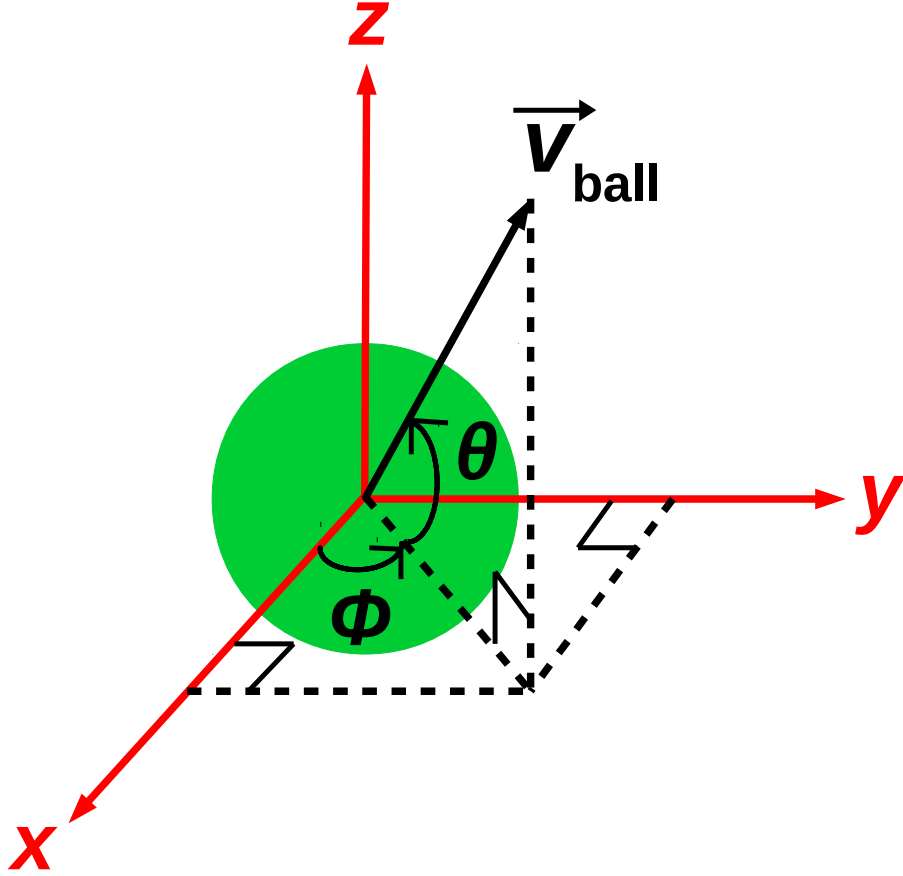

Figure 19: The projection of velocity vector for a golf ball on three-dimensional basis $(\hat{x}, \hat{y}, \hat{z})$. We define θ is the elevation angle from the horizontal ground, and ϕ is the direction angle counter-clockwise with respect to the rotational $\hat{z}$ axis.
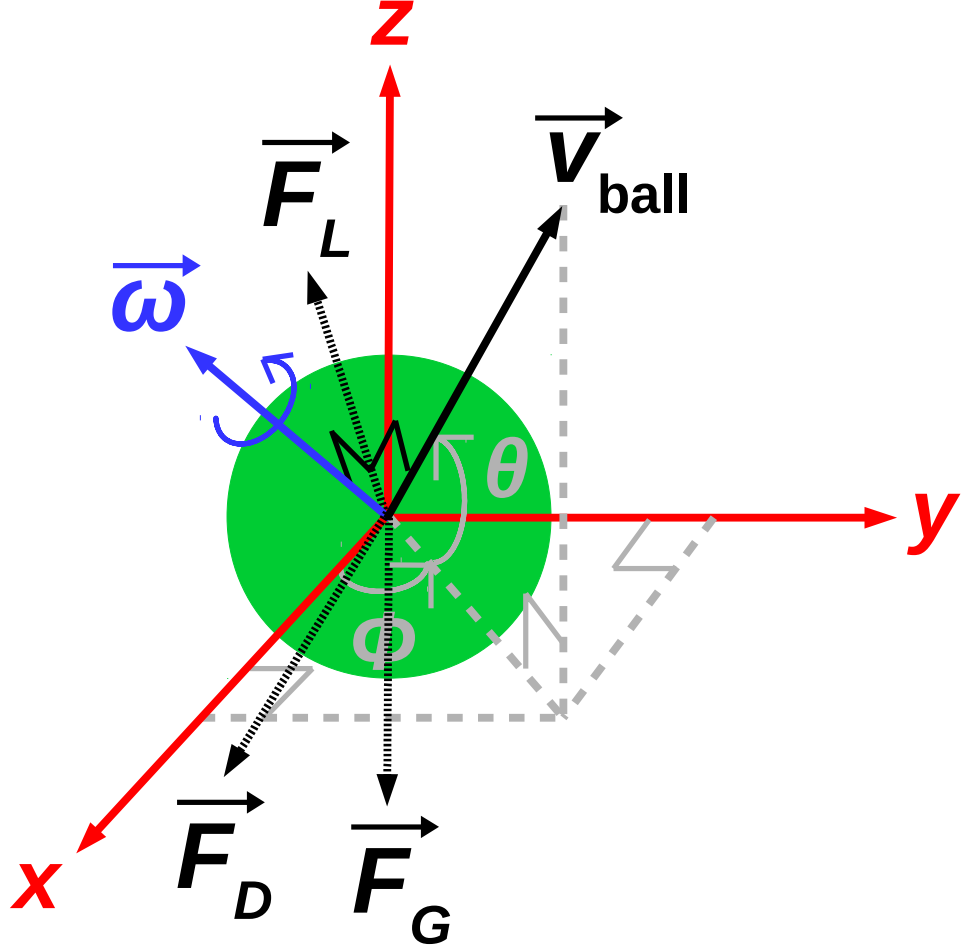
Figure 20: The vectors of ball velocity $\overrightarrow{v}_{\text{ball}}$, gravitation $\overrightarrow{F_G}$, drag force $\overrightarrow{F_D}$, angular velocity $\overrightarrow{w}$ and lift force $\overrightarrow{F_L}$ on a golf ball.

Let the vector of wind velocity is $\overrightarrow{v}_{\text{wind}} = v_{\text{wind},x}\hat{x} + v_{\text{wind},y}\hat{y} + v_{\text{wind},z}\hat{z}$, where

$$\begin{cases} v_{\text{wind},x} = v_{\text{wind}} \cdot \cos\theta_{\text{wind}} \cdot \cos\phi_{\text{wind}}; \\ v_{\text{wind},y} = v_{\text{wind}} \cdot \cos\theta_{\text{wind}} \cdot \sin\phi_{\text{wind}}; \\ v_{\text{wind},z} = v_{\text{wind}} \cdot \sin\theta_{\text{wind}}, \end{cases}$$

(35)

$$\text{and} \quad v_{\text{wind}} = |\overrightarrow{v}_{\text{wind}}| = \sqrt{v_{\text{wind},x}^2 + v_{\text{wind},y}^2 + v_{\text{wind},z}^2} \ .$$

θ_{wind} and ϕ_{wind} are represented as elevation and direction angles for wind. Since the air stream velocity is $\overrightarrow{U} = -\overrightarrow{v}_{\text{ball}} + \overrightarrow{v}_{\text{wind}}$, the unit vector of drag force is equal to $\overrightarrow{U}$, i.e.,

$$\frac{\overrightarrow{F_D}}{|\overrightarrow{F_D}|} = \frac{\overrightarrow{U}}{|\overrightarrow{U}|}, \quad \text{and} \quad |\overrightarrow{F_D}| = C_D\left(Re, \frac{|\overrightarrow{V}|}{|\overrightarrow{U}|}\right) A\rho_{\text{air}}\frac{\overrightarrow{U}^2}{2}.$$

(36)

Let the vector of golf ball rotational angular velocity is $\vec{w} = w_x\hat{x} + w_y\hat{y} + w_z\hat{z}$, where

$$\begin{cases} w_x = w \cdot \cos\theta_w \cdot \cos\phi_w; \\ w_y = w \cdot \cos\theta_w \cdot \sin\phi_w; \\ w_z = w \cdot \sin\theta_w, \end{cases} \tag{37}$$

$$\text{and} \quad w = |\vec{w}| = \sqrt{w_x^2 + w_y^2 + w_z^2} \ .$$

θ_w and ϕ_w are represented as elevation and direction angles for rotational angular velocity. The circumferential (rotational) velocity of a golf ball is $\vec{V} = \vec{w} \times \vec{R}$, where $|\vec{R}|$ is the radius of ball. $\vec{w}$ and $\vec{R}$ are orthogonal vectors with each other. The direction of lift force is the cross product of unit vectors of air stream and rotational angular velocity

$$\frac{\vec{F_L}}{|\vec{F_L}|} = \frac{\vec{U}}{|\vec{U}|} \times \frac{\vec{w}}{|\vec{w}|}, \quad \text{and} \quad |\vec{F_L}| = C_L \left(\frac{|\vec{V}|}{|\vec{U}|} \right) A\rho_{\text{air}} \frac{\vec{U}^2}{2}. \tag{38}$$

The gravitation direction is on the minus of vertical vector: $\vec{F_G} = -mg\hat{z}$, where m is the mass of a golf ball and $g = 9.806$ m/sec^2 is the gravitational acceleration.

So, if we know the vectors of ball velocity $\vec{v}_{\text{ball}}$, wind velocity $\vec{v}_{\text{wind}}$ and rotational angular velocity $\vec{w}$, we can calculate $\vec{F_D}$ and $\vec{F_L}$ by Eq. 33 $\sim$ Eq. 38. The total force on a flying golf ball is $\vec{F}_{\text{total}} = \vec{F_D} + \vec{F_L} + \vec{F_G}$. Let the acceleration vector of ball is $\vec{a}$, which can be calculated by $\vec{F}_{\text{total}} = m\vec{a}$. If we let the vectors of drag force $\vec{F_D} = F_{D,x}\hat{x} + F_{D,y}\hat{y} + F_{D,z}\hat{z}$ and lift force $\vec{F_L} = F_{L,x}\hat{x} + F_{L,y}\hat{y} + F_{L,z}\hat{z}$, the acceleration vector of ball is expressed as $\vec{a} = \mathbf{a_x}\hat{x} + \mathbf{a_y}\hat{y} + \mathbf{a_z}\hat{z}$, where

$$\begin{cases} \mathbf{a_x} = \dfrac{1}{m}(F_{D,x} + F_{L,x}); \\ \mathbf{a_y} = \dfrac{1}{m}(F_{D,y} + F_{L,y}); \\ \mathbf{a_z} = \dfrac{1}{m}(F_{D,z} + F_{L,z}) - g. \end{cases} \tag{39}$$

These accelerations are as functions of vectors $\vec{v}_{\text{ball}}$, $\vec{v}_{\text{wind}}$ and $\vec{w}$, i.e.,

$$\begin{cases} \mathbf{a_x} \to \mathbf{a_x}(v_{\text{ball,x}}, v_{\text{ball,y}}, v_{\text{ball,z}}, v_{\text{wind,x}}, v_{\text{wind,y}}, v_{\text{wind,z}}, w_x, w_y, w_z); \\ \mathbf{a_y} \to \mathbf{a_y}(v_{\text{ball,x}}, v_{\text{ball,y}}, v_{\text{ball,z}}, v_{\text{wind,x}}, v_{\text{wind,y}}, v_{\text{wind,z}}, w_x, w_y, w_z); \\ \mathbf{a_z} \to \mathbf{a_z}(v_{\text{ball,x}}, v_{\text{ball,y}}, v_{\text{ball,z}}, v_{\text{wind,x}}, v_{\text{wind,y}}, v_{\text{wind,z}}, w_x, w_y, w_z), \end{cases} \tag{40}$$

We can apply fourth-order Runge-Kutta method to calculate the ball trajectory in three-dimension. Assuming the vectors of wind velocity $\vec{v}_{\text{wind}}$ and rotational angular velocity of a ball $\vec{w}$ are constants during the fly. For the ball velocity changed with time, $\vec{v}_{\text{ball}} \to \vec{v}(t) =$

$v_x(t)\hat{x} + v_y(t)\hat{y} + v_z(t)\hat{z}$, which is calculated step-by-step with Runge-Kutta method:

$$
\begin{cases}
t_{n+1} & = t_n + h; \\
v_{x,n+1} & = v_{x,n} + \dfrac{h}{6}(k_{1,x} + 2k_{2,x} + 2k_{3,x} + k_{4,x}); \\
v_{y,n+1} & = v_{y,n} + \dfrac{h}{6}(k_{1,y} + 2k_{2,y} + 2k_{3,y} + k_{4,y}); \\
v_{z,n+1} & = v_{z,n} + \dfrac{h}{6}(k_{1,z} + 2k_{2,z} + 2k_{3,z} + k_{4,z}),
\end{cases}
$$

$$
\text{where} \quad
\begin{cases}
k_{1,x} = \mathbf{a_x}(v_{x,n},\ v_{y,n},\ v_{z,n},\ \cdots); \\
k_{1,y} = \mathbf{a_y}(v_{x,n},\ v_{y,n},\ v_{z,n},\ \cdots); \\
k_{1,z} = \mathbf{a_z}(v_{x,n},\ v_{y,n},\ v_{z,n},\ \cdots);
\end{cases}
$$

$$
\text{and} \quad
\begin{cases}
k_{2,x} = \mathbf{a_x}(v_{x,n}+\frac{1}{2}k_{1,x}h,\ v_{y,n}+\frac{1}{2}k_{1,y}h,\ v_{z,n}+\frac{1}{2}k_{1,z}h,\cdots); \\
k_{2,y} = \mathbf{a_y}(v_{x,n}+\frac{1}{2}k_{1,x}h,\ v_{y,n}+\frac{1}{2}k_{1,y}h,\ v_{z,n}+\frac{1}{2}k_{1,z}h,\cdots); \\
k_{2,z} = \mathbf{a_z}(v_{x,n}+\frac{1}{2}k_{1,x}h,\ v_{y,n}+\frac{1}{2}k_{1,y}h,\ v_{z,n}+\frac{1}{2}k_{1,z}h,\cdots),
\end{cases}
$$

$$
\text{and} \quad
\begin{cases}
k_{3,x} = \mathbf{a_x}(v_{x,n}+\frac{1}{2}k_{2,x}h,\ v_{y,n}+\frac{1}{2}k_{2,y}h,\ v_{z,n}+\frac{1}{2}k_{2,z}h,\ \cdots); \\
k_{3,y} = \mathbf{a_y}(v_{x,n}+\frac{1}{2}k_{2,x}h,\ v_{y,n}+\frac{1}{2}k_{2,y}h,\ v_{z,n}+\frac{1}{2}k_{2,z}h,\ \cdots); \\
k_{3,z} = \mathbf{a_z}(v_{x,n}+\frac{1}{2}k_{2,x}h,\ v_{y,n}+\frac{1}{2}k_{2,y}h,\ v_{z,n}+\frac{1}{2}k_{2,z}h,\ \cdots),
\end{cases}
$$

$$
\text{and} \quad
\begin{cases}
k_{4,x} = \mathbf{a_x}(v_{x,n}+k_{3,x}h,\ v_{y,n}+k_{3,y}h,\ v_{z,n}+k_{3,z}h,\ \cdots); \\
k_{4,y} = \mathbf{a_y}(v_{x,n}+k_{3,x}h,\ v_{y,n}+k_{3,y}h,\ v_{z,n}+k_{3,z}h,\ \cdots); \\
k_{4,z} = \mathbf{a_z}(v_{x,n}+k_{3,x}h,\ v_{y,n}+k_{3,y}h,\ v_{z,n}+k_{3,z}h,\ \cdots).
\end{cases}
\tag{41}
$$

h is a small value of time interval (say $h = 0.001$ sec) and n is the n-th step of iterations. Then we can calculate the position of ball changed with time:

$$
\begin{cases}
x_{n+1} = x_n + \left(\dfrac{v_{x,n} + v_{x,n+1}}{2}\right) h; \\
y_{n+1} = y_n + \left(\dfrac{v_{y,n} + v_{y,n+1}}{2}\right) h; \\
z_{n+1} = z_n + \left(\dfrac{v_{z,n} + v_{z,n+1}}{2}\right) h,
\end{cases}
\tag{42}
$$

so the trajectory of a flying golf ball is obtained.

3.3 Simulation Studies

Now we demonstrate some simulations for golf ball flight trajectories. The basic settings of parameters for golf ball and environmental conditions are listed in Table 5.

Table 5: The basic parameters for golf ball trajectory simulations.

Golf ball parameter	Value
Mass (kg)	0.0458
Diameter (m)	0.0428
Drag coefficient C_D	0.285
Lift coefficient C_L	0.1
Golf ball launch condition	**Value**
Launch speed (m/sec)	45
Launch elevation angle θ (degree)	15
Launch direction angle ϕ (degree)	0
Spin elevation angle θ_w (degree)	0
Spin direction angle ϕ_w (degree)	-90
Environmental condition	**Value**
Air density (kg/m^3)	1.2
Wind speed (m/sec)	0
Wind elevation angle θ_{wind} (degree)	...
Wind direction angle ϕ_{wind} (degree)	...

3.3.1 Case 7: The Effect of Drag and Lift Coefficients

Although the drag and lift parameters are changed with the ratio of golf ball rotational speed to the stream speed, $|\overrightarrow{V}|/|\overrightarrow{U}|$, as shown an example in Figure 18. Here we assume they are constants in order to see their effects on the flight trajectories and distances. Using the parameter settings in Table 5, we vary the $C_D = 0.1 \sim 0.6$ and $C_L = 0 \sim 0.3$ to simulate their trajectories and obtain flight distances, which are shown in Figure 21 and Figure 22. From simulations we see the flight distance is roughly proportional to $1/C_D$ and C_L (for $\theta_w = 0°$ and $\phi_w = -90°$).
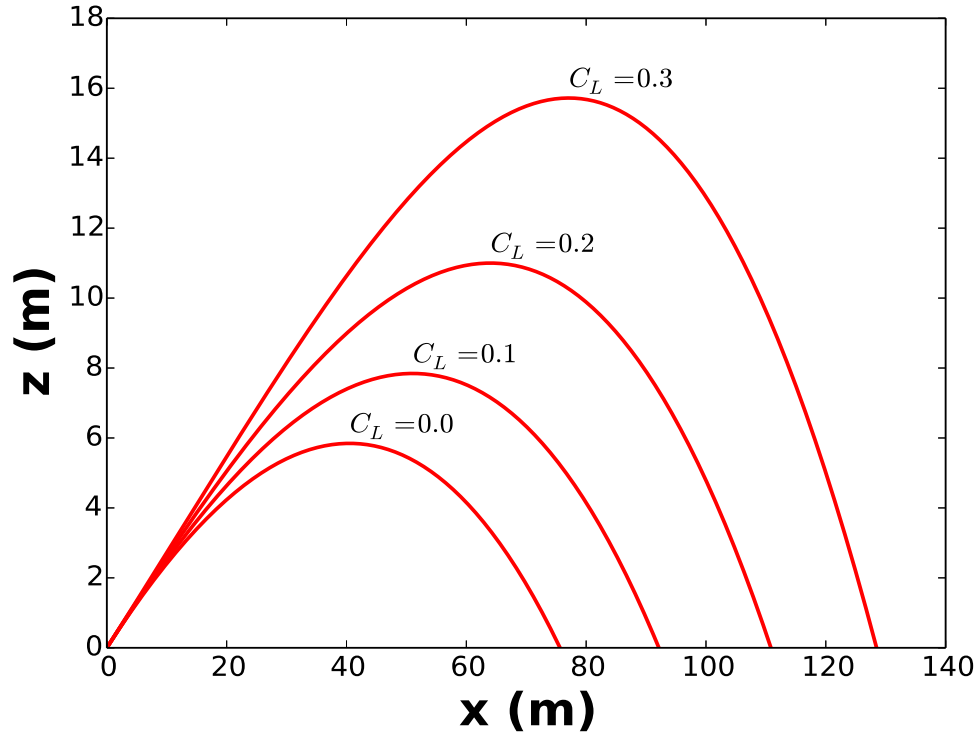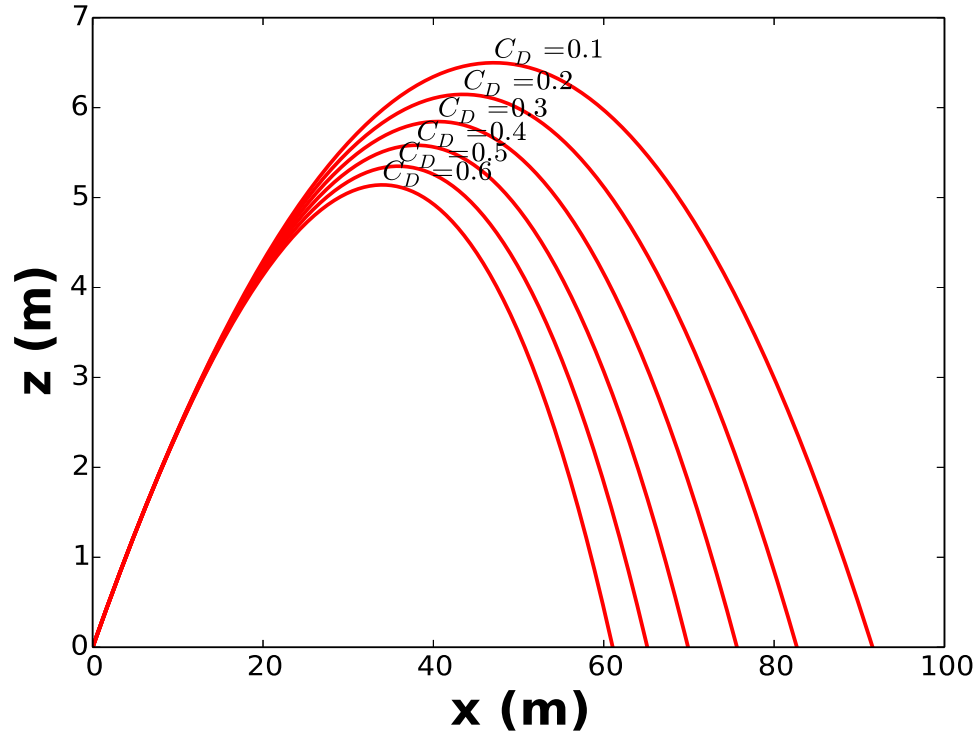
Figure 21: Upper plot shows the trajectories of a golf ball with $C_D = 0.1 \sim 0.6$ and $C_L = 0$. Lower plot shows the trajectories of a golf ball with $C_L = 0 \sim 0.3$ (for $\theta_w = 0°$ and $\phi_w = -90°$) and $C_D = 0.3$.

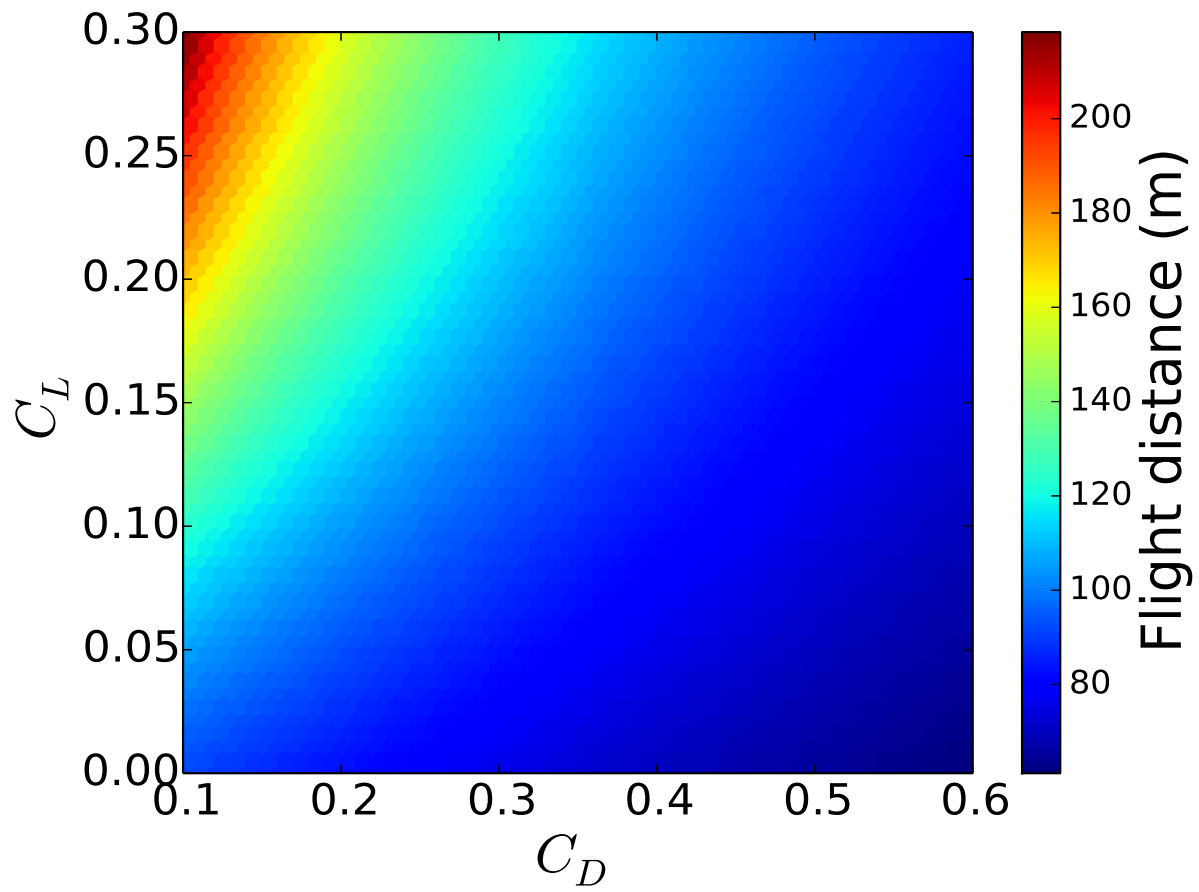Figure 22: The heat map of flight distances for different C_L (for $\theta_w = 0°$ and $\phi_w = -90°$) and C_D settings of a golf ball.

3.3.2 Case 8: The Effect of Launch Elevation Angle

Using the parameter settings in Table 5, now we change the golf ball launch elevation angle $\theta = 0° \sim 90°$ with different $C_D = 0.1 \sim 0.6$ or $C_L = 0 \sim 0.3$ in simulations. The results are shown in Figure 23.

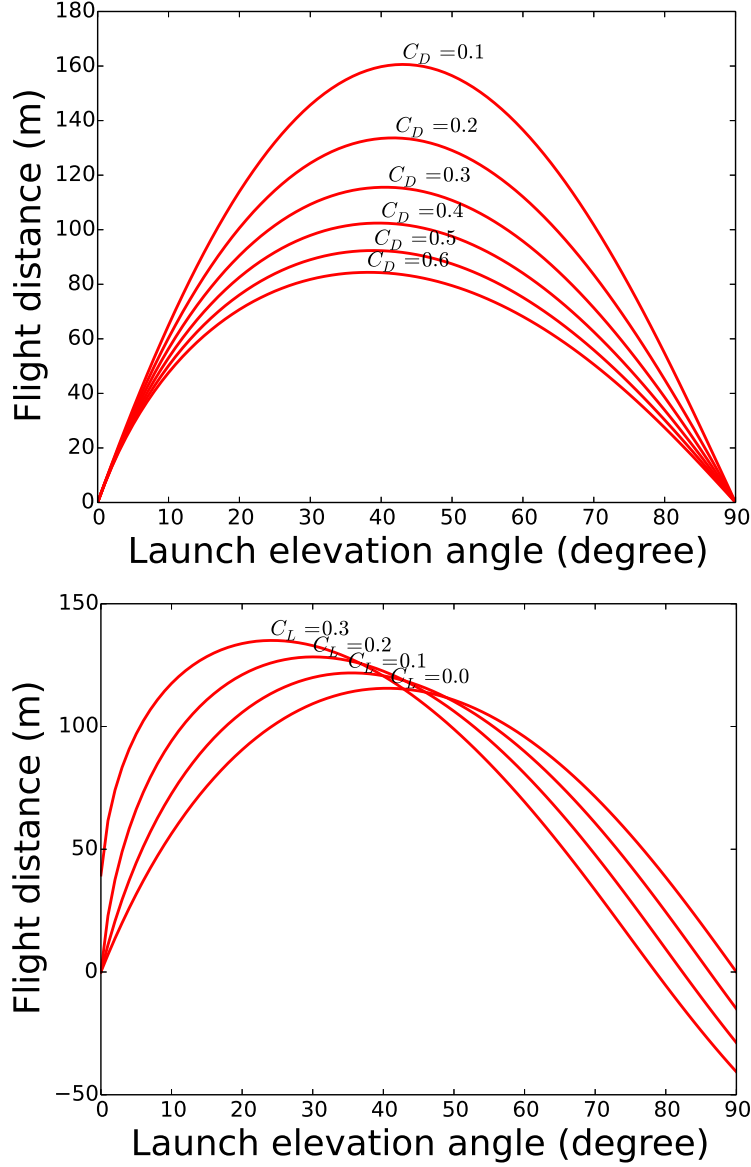Figure 23: Upper plot shows the flight distance vs. launch elevation angle of a golf ball with $C_D = 0.1 \sim 0.6$ and $C_L = 0$. Lower plot shows the flight distance vs. launch elevation angle of a golf ball with $C_L = 0 \sim 0.3$ (for $\theta_w = 0°$ and $\phi_w = -90°$) and $C_D = 0.3$. Note that the negative value of flight distance means the drop location of a golf ball is behind the golfer.

3.3.3 Case 9: The Effect of Spin Direction

Using the parameter settings in Table 5, now we change the golf ball spin direction $\theta_w = 0° \sim 360°$ with $\phi_w = -90°$. The simulation results are shown in Figure 24.
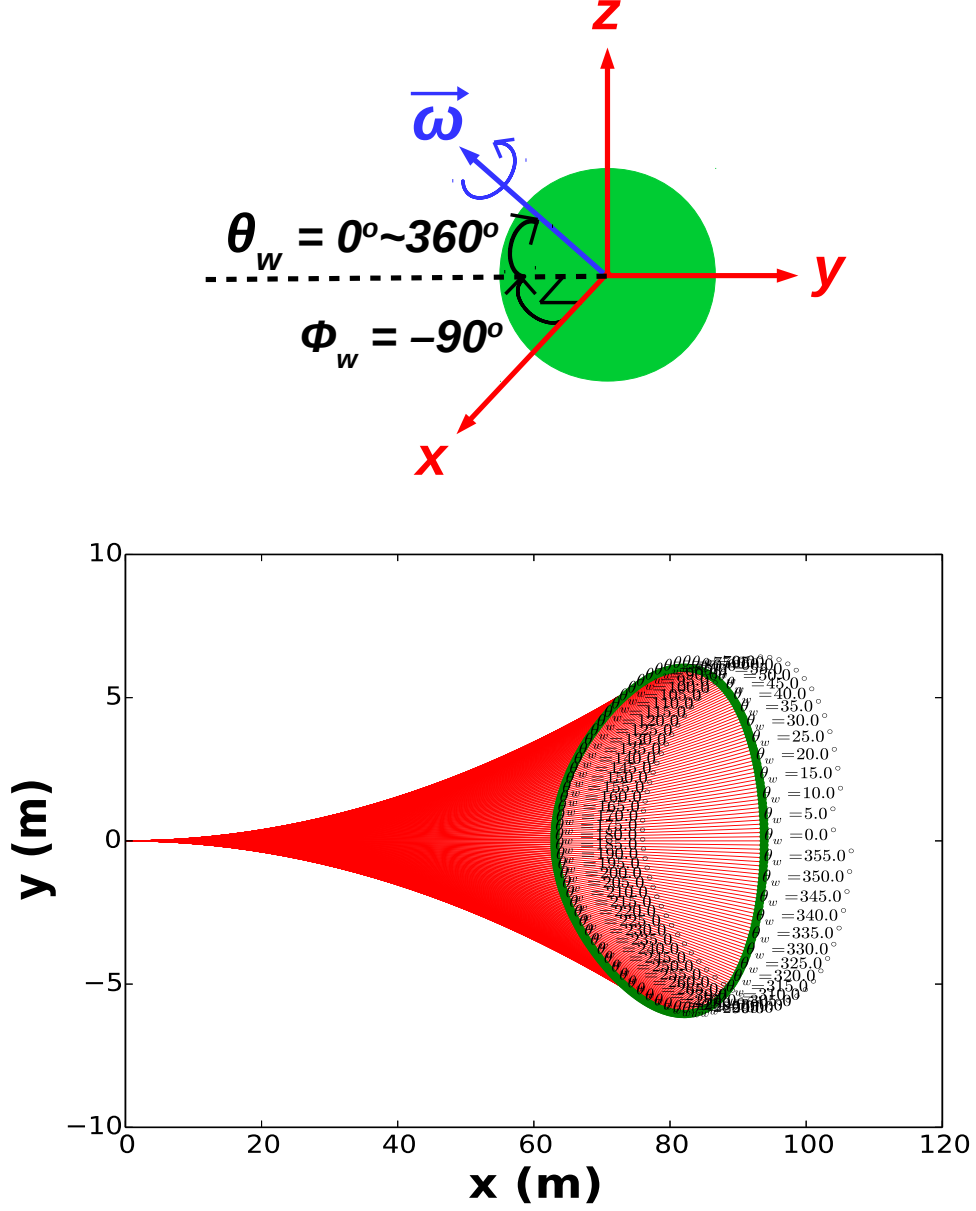

Figure 24: Upper plot shows the spin direction of a golf ball. Lower plot shows the simulation trajectories (red lines) and the drop positions (green solid circles) of a golf ball on horizontal x-y plane (for $\theta_w = 0° \sim 360°$ and $\phi_w = -90°$).

3.3.4 Case 10: The Effect of Wind

Using the same parameter settings in Table 5, now we add the wind speed 5 (m/sec) on the directions $\theta_{\text{wind}} = 0°$ and $\phi_{\text{wind}} = [0°, 90°, 180°, 270°]$. The simulation results are shown in Figure 25.
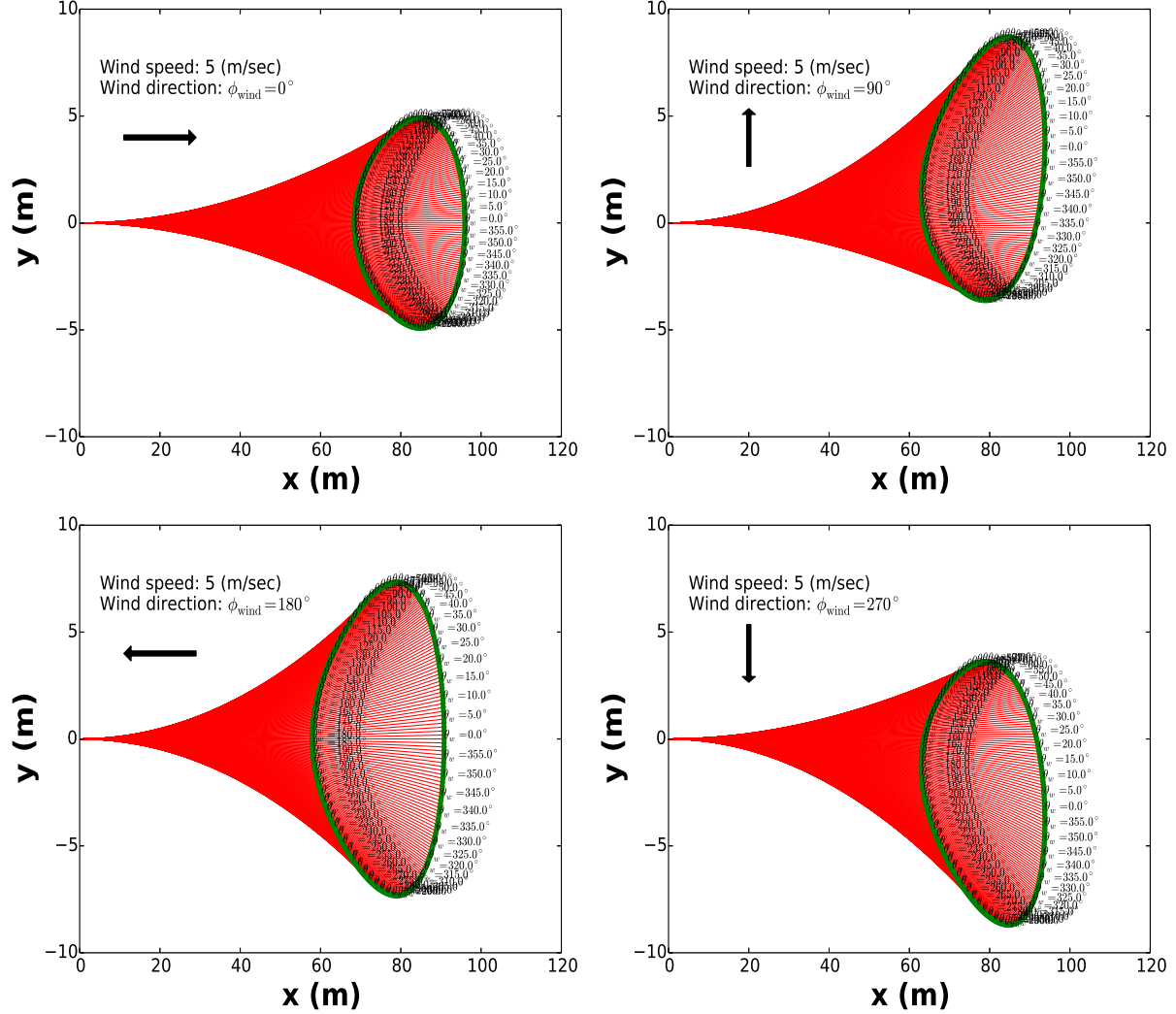
Figure 25: Assuming the wind speed is 5 (m/sec), the effects of wind force on golf ball trajectories on x-y plane are shown with the wind direction: $\phi_{\text{wind}} = 0°$ (upper left), $\phi_{\text{wind}} = 90°$ (upper right), $\phi_{\text{wind}} = 180°$ (lower left) and $\phi_{\text{wind}} = 270°$ (lower right). Note that we set $\theta_{\text{wind}} = 0°$, the red lines are simulation trajectories and the green solid circles are drop positions for different spin direction ($\theta_w = 0° \sim 360°$ with $\phi_w = -90°$) of a golf ball.

4 USER'S GUIDE

4.1 Installation

The Simple Golf Simulator is written in Python language, which is easy to understand, modify and install in different OS platforms of computers. Before running the program, the user has to install the basic Python package (version 2.7.6 or above) [10], NumPy [11] and Matplotlib [12]. These Python packages are open source codes and they are free to download and use.

The main files of Simple Golf Simulator are **AppFunc.py**, **AppFunc2.py**, **BasicFunc.py**, **BasicFunc2.py**, **Plot.py**, **Plot2.py** and **Main.py**. One has to put these main files in the same directory while running. The other files **Case1.py**, **Case2.py**, ..., **Case10.py** are demonstrations of simulations which are shown in the Sec. 2.5 and Sec. 3.3. Users can learn how to call the sub-functions of Simple Golf Simulator to do their own study from these demonstration files. To start the main program, one has to execute the file **Main.py** by the following comment in the terminal:

$ python Main.py

For Linux user, one can also make **Main.py** as an executable file by

$ chmod a+x Main.py

and then execute **Main.py** directly:

$ ./Main.py

If success, the main control panel will be shown like Figure 26. The Left column of panel is for golf swing simulation, and right column of panel is for golf ball trajectory simulation. In the same way, we can make the files **Case1.py** ∼ **Case10.py** executable. For example:

$ chmod a+x Case1.py

and then execute **Case1.py** directly:

$ ./Case1.py

In this report the Simple Golf Simulator is operated under the Linux system.

The Simple Golf Simulator (Copyright @ 2016 C.-C. Chiang)

(I) Set golfer parameters

1. Gender:	Male
2. Weight (kg):	70.0
3. Shoulder radius (m):	0.17
4. Arm length (m):	0.6

(II) Set club parameters

5. Head mass (kg):	0.2
6. Shaft mass (kg):	0.1
7. Head length (m):	0.1
8. Shaft length (m):	1.0

(III) Set swing conditions

9. Swing plane angle (degree):	60
10. Initial arm angle (degree):	135
*11. Impact arm angle (degree):	0
12. Initial wrist-cock angle (degree):	120
*13. Impact wrist-cock angle (degree):	0
*14. Horizontal acceleration (m/sec^2):	0
*15. Vertical acceleration (m/sec^2):	0
16. Choose swing type:	Type I

(IV) Set swing torques

17. Arm torque (N-m):	100
*18. Raising time of arm torque (sec):	0.01
19. Wrist-cock torque (N-m):	N/A
**20. At which arm angle the wrist-cock torque started (degree):	135

(**) The angle in item 20 should be equal or smaller than the initial arm angle in item 10.

*21. Raising time of wrist-cock torque (sec):	0.01
*22. Minimum of wrist-cock torque (N-m):	-50
*23. Maximum of wrist-cock torque (N-m):	0

Click to optimize wrist-cock torque (fast)

Click to optimize wrist-cock torque (complete)

(V) Simulate the swing

24. Choose simulation method:	Solution 3

25. Choose the results to plot:

☐ Tracks   ☐ Angles

☐ Angular velocities   ☐ Angular accelerations

☐ Clubhead velocity   ☐ Torques

☐ Arm length   ☐ 1st and 2nd moments

26. Clubhead impact velocity (m/sec):	N/A
27. Systematic error of clubhead impact velocity (m/sec):	N/A
28. Clubhead impact angle (degree):	N/A
29. Systematic error of clubhead impact angle (degree):	N/A

Click to simulate / plot golf swing

(VI) Set golf ball parameters

30. Mass (kg):	0.0458
31. Diameter (m):	0.0428
32. COR:	0.775
33. Drag coefficient:	0.285
34. Lift coefficient:	0.1

(VII) Set environmental conditions

*35. Air density (kg/m^3):	1.2
36. Wind speed (absolute value) (m/sec):	0
37. Wind elevation angle:	0
38. Wind direction angle:	0

(VIII) Set launch conditions of golf ball

39. Loft angle of clubhead (degree):	15
40. Launch speed (absolute value) (m/sec):	N/A
41. Launch elevation angle (degree):	N/A
*42. Launch direction angle (degree):	0
43. Spin elevation angle (degree):	0
44. Spin direction angle (degree):	-90

Click to calculate golf ball launch speed and elevation angle
(based on clubhead impact velocity and loft angle)

(IX) Simulate the golf ball trajectory

*45. Altitude of target (m):	0

46. Choose the results to plot:

☐ X-Z   ☐ X-Y

☐ Y-Z   ☐ X-Y-Z (3-D plot)

47. Drop location in X (m):	N/A
48. Drop location in Y (m):	N/A
49. Flight distance in X-Y plane (m):	N/A

Click to simulate / plot golf ball trajectory

(*) The suggested default value.

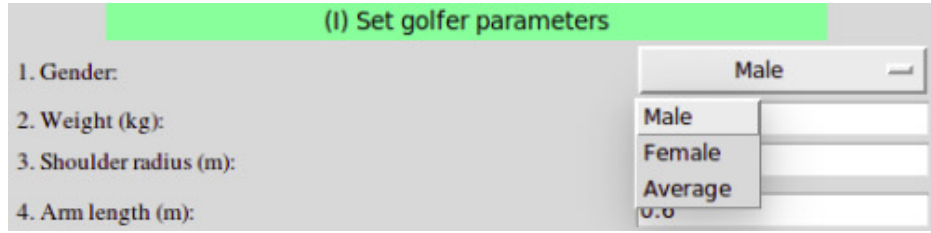Figure 26: The main control panel of Simple Golf Simulator.

41

4.2 The Main Control Panel

In the main control panel, the default values are already filled in the white blanks. Users can change the default values for their own study. The yellow blank is to be automatically filled by clicking the yellow button, which should be done after we set parameters in the white blanks. Users can also set their own values in the yellow blank for special studies. The blue blank is to be automatically filled by clicking the blue button, which shows the simulation results and it should be done after we have set parameters in the white and yellow blanks. Users can just follow the item number, form top to bottom and left to right, step-by-step to set parameters for simulations.

The descriptions of items are below:

1. **Gender:**
   The golfer's gender. User can choose **Male**, **Female** or **Average**. The percentages of weights of upper arm, forearm and hand are dependent on golfer's gender, as shown in Table 2, Sec. 2.2. So it will affect the values of first and second moments of golfer's arm.

2. **Weight (kg):**
   The golfer's weight.

3. **Shoulder radius (m):**
   The golfer's shoulder radius, as show the R_S in Figure 6, Sec. 2.2.

4. **Arm length (m):**
   The golfer's arm length, as show the R_A in Figure 6, Sec. 2.2.

5. **Head mass (kg):**
   Clubhead mass of the club.

6. **Shaft mass (kg):**
   Shaft mass of the club.

7. **Head length (m):**
   The length of clubhead, as shown the L_{head} in Figure 7, Sec. 2.3.

8. **Shaft length (m):**
   The length of shaft, as shown the L_{head} in Figure 7, Sec. 2.3.

9. **Swing plane angle (degree):**
   As shown the ϕ angle in Figure 3, Sec. 2.1.

10. **Initial arm angle (degree):**
    The start angle of arm $\theta \rightarrow \theta_0$, which is shown in Figure 2, Sec. 2.1.

11. **Impact arm angle (degree):**
    The final angle of of arm $\theta \to \theta_f$, at which the clubhead impacted on the golf ball.

12. **Initial wrist-cock angle (degree):**
    The start angle of wrist-cock $\beta \to \beta_0$, which is shown in Figure 2, Sec. 2.1.

13. **Impact wrist-cock angle (degree):**
    The final angle of wrist-cock $\beta \to \beta_f$, at which the clubhead impacted on the golf ball.
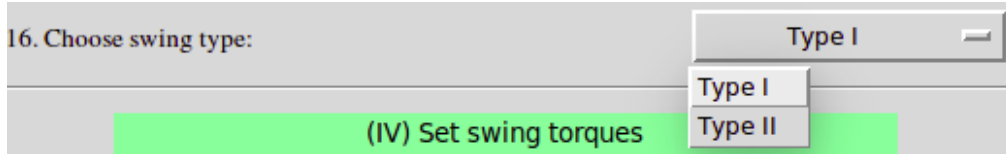
14. **Horizontal acceleration (m/sec^2):**
    As shown the a_x in Figure 2, Sec. 2.1.

15. **Vertical acceleration (m/sec^2):**
    As shown the a_y in Figure 2, Sec. 2.1. Note that we define the direction of positive of a_y is toward down to the ground.

16. **Choose swing type:**
    User can choose the type of backswing, **Type I: restricted backswing** or **Type II: full-length backswing**, which is shown in Figure 5, Sec. 2.2.

17. **Arm torque (N-m):**
    The Q_α in Figure 2, Sec. 2.1. Note that we define the direction of positive Q_α is counter-clockwise in the swing plane.

18. **Raising time of arm torque (sec):**
    The τ_{Q_α} value in Eq. 28, Sec. 2.5.

19. **Wrist-cock torque (N-m):**
    The Q_β in Figure 2, Sec. 2.1. Note that we define the direction of positive Q_β is clockwise in the swing plane.

20. **At which arm angle the wrist-cock torque started (degree):**
    The $t_{\theta=?}$ value in Eq. 28, Sec. 2.5. Note that the angle we choose should be equal or less than the θ_0 value (in **item 10**).

21. **Raising time of wrist-cock torque (sec):**
    The τ_{Q_β} value in Eq. 28, Sec. 2.5.

22. **Minimum of wrist-cock torque (N-m):**
    Set the minimum of wrist-cock torque Q_β, which is used for optimization.

23. **Maximum of wrist-cock torque (N-m):**
    Set the maximum of wrist-cock torque Q_β, which is used for optimization.

Button :

<div style="text-align: center">

**Click to optimize wrist-cock torque (fast)**

Click to optimize wrist-cock torque (complete)

</div>

Given the arm torque in **item 17**, impact arm and wrist-cock angles in **item 11** and **item 13**, we need to search for the best wrist-cock torque in the range between **item 22** and **item 23**, in order to fit the swing requirements. The upper (fast) button will scan the wrist-cock torque from maximum to the optimized value. The lower (complete) button will scan the wrist-cock torque from maximum to the value beyond the optimized one by -10 (N-m). The plots β vs. $-Q_\beta$ and $-d\beta/dQ_\beta$ vs. $-Q_\beta$ will be shown after the scan is finished. The optimized wrist-cock torque will also be re-filled in **item 19**.
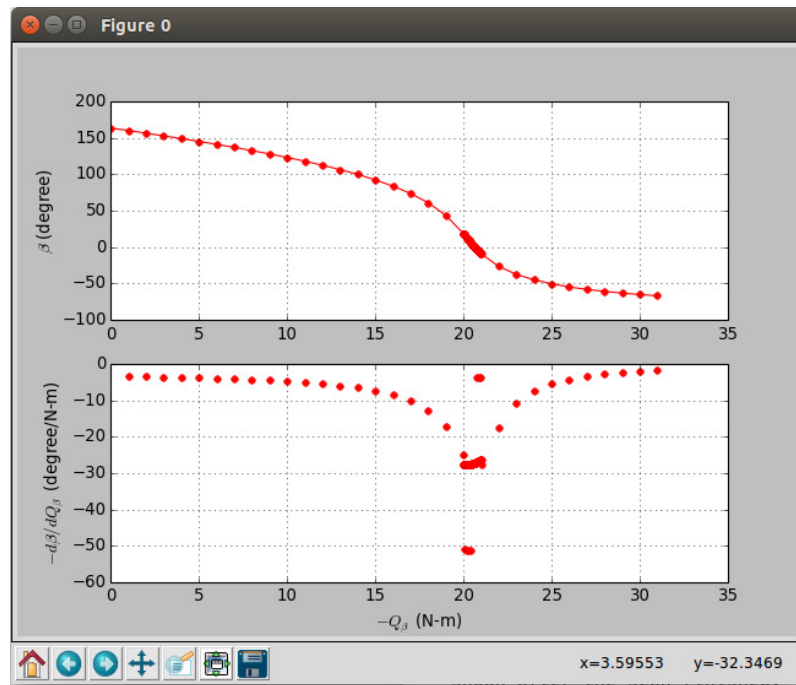
24. Choose simulation method:

User can choose **Solution 1**, **Solution 2** or **Solution 3** for swing simulation, their explanations shown in Sec. 2.4. The default is **Solution 3** (suggestion).
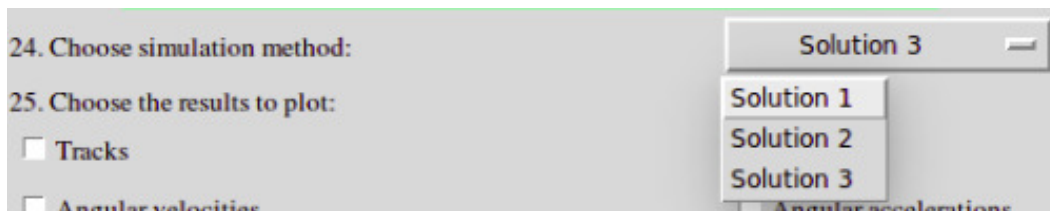
25. Choose the results to plot:

User can choose which simulation result to plot by clicking the following check boxes:

☐ **Tracks**: like the plot in Figure 9 (top left), Sec. 2.5.

<div style="text-align: center">

44

</div>

☐ **Angles**: like the plot in Figure 9 (top right), Sec. 2.5.

☐ **Angular velocities**: like the plot in Figure 9 (middle left), Sec. 2.5.

☐ **Angular accelerations**: like the plot in Figure 9 (middle right), Sec. 2.5.

☐ **Clubhead velocity**: like the plot in Figure 9 (bottom left), Sec. 2.5.

☐ **Torques**: like the plot in Figure 9 (bottom right), Sec. 2.5.

☐ **Arm length**: like the plot in Figure 8 (right), Sec. 2.5.

☐ **1st and 2nd moments**: like the plot in Figure 8 (left), Sec. 2.5.

26. **Clubhead impact velocity (m/sec):**
    The clubhead speed while impacts on a golf ball.

27. **Systematic error of clubhead impact velocity (m/sec):**
    The changes of clubhead speed from the **item 26** while we vary the wrist-cock torque Q_β with ± 0.01 (N-m) from the nominate value in **item 19**.

28. **Clubhead impact angle (degree):**
    The clubhead velocity angle $\theta_{\overrightarrow{V_C}}$ while impacts on a golf ball. The definition of $\theta_{\overrightarrow{V_C}}$ can be found in Eq. 4, Sec. 2.1, which is an elevation angle.

29. **Systematic error of clubhead impact angle (degree):**
    The changes of clubhead velocity angle from the **item 28** while we vary the wrist-cock torque Q_β with ± 0.01 (N-m) from the nominate value in **item 19**.

$\boxed{\textbf{Button}}$:

Click to simulate / plot golf swing

Click to simulate the golf swing and the result values will be filled in **item 26** ∼ **item 29**.

30. **Mass (kg):**
    The golf ball mass.

31. **Diameter (m):**
    The golf ball diameter.

32. **COR:**
    The coefficient of rebound for a golf ball.

33. **Drag coefficient:**
    The C_D value which is defined in Eq. 31, Sec. 3.1

34. **Lift coefficient:**
    The C_L value which is defined in Eq. 31, Sec. 3.1

35. **Air density (kg/m^3):**
    The density of air, which is dependent on weather conditions or altitude.

36. Wind speed (absolute value) (m/sec):
    The speed of wind, which is a 0 or positive value.

37. Wind elevation angle:
    The θ_{wind}, which is defined in Eq. 35, Sec. 3.2.

38. Wind direction angle:
    The ϕ_{wind}, which is defined in Eq. 35, Sec. 3.2.

39. Loft angle of clubhead (degree):
    The loft angle on clubhead is usually an elevation angle that gives to a golf ball.

40. Launch speed (absolute value) (m/sec):
    The launch speed of a golf ball, which is a 0 or positive value.

41. Launch elevation angle (degree):
    The θ, which is defined in Figure 19, Sec. 3.2.

42. Launch direction angle (degree):
    The ϕ, which is defined in Figure 19, Sec. 3.2.

43. Spin elevation angle (degree):
    The θ_w, which is defined in Eq. 37, Sec. 3.2.

44. Spin direction angle (degree):
    The ϕ_w, which is defined in Eq. 37, Sec. 3.2.

| Button |:

> Click to calculate golf ball launch speed and elevation angle
> (based on clubhead impact velocity and loft angle)

The launch speed of a golf ball is calculated by clubhead impact velocity in **item 26** and COR in **item 32** with the Eq. 30 in Sec. 2.5. The launch elevation angle of a golf ball is calculated by the clubhead impact angle in **item 28** plus the loft angle on clubhead in **item 39**. The **item 40** and **item 41** will be re-filled after the calculation is finished.

45. Altitude of target (m):
    The altitude of target compared to the golf ball launch point. The default value is 0.

46. Choose the results to plot:
    User can choose which simulation result to plot by clicking the following check boxes:

    ☐ **X-Z**: The simulation track of a golf ball in horizontal-vertical space, like the Figure 21 in Sec. 3.3.

    ☐ **X-Y**: The simulation track of a golf ball in horizontal-vertical space, like the Figure 24 in Sec. 3.3.

    ☐ **Y-Z**: The simulation track of a golf ball in horizontal-vertical space.

□ **X-Y-Z (3-D plot)**: The simulation track of a golf ball in 3-D space.

47. Drop location in X (m):

The drop location in x, assuming the launch position of a golf ball is $x = 0$.

48. Drop location in Y (m):

The drop location in y, assuming the launch position of a golf ball is $y = 0$.

49. Flight distance in X-Y plane (m):

The flight distance in horizontal space. It is usually a positive value, negative value means the drop location of a golf ball is behind the golfer.

Button :

Click to simulate / plot golf ball trajectory

Click to simulate the golf ball trajectory. The result values will be filled in **item 47** ∼ **item 49**.

5 SUMMARY

The Simple Golf Simulator should be verified by experimental data. There are a lot of variables in the golf swing model and golf ball flight trajectory. They can be very different with different golfers, clubs, swing types and golf balls they use. However through the simulation and analysis of the data, we can understand the mechanism behind it and provide valuable information to optimize the performance for a golfer. It may be also helpful in the design of product specs for the club or golf ball. There are some works to be done to improve this simulation program. It is better to rely on the real world data. For the golf club swing model:

- The functions of arm and wrist-cock torques with respect to the time during the swing may be different for golfers. In such case, we have to re-model the Eq. 28 in Sec. 2.5.

- The function of arm bending angle for Type II (full-length) backswing with respect to the time during the swing may be different for golfers. In such case, we have to re-model the Eq. 29 in Sec. 2.5.

- The flexibility of a club shaft may need to be considered.

- The first and second moments of golfer's arm or club may need to be re-calculated for special cases.

- ...

For the golf ball flight trajectory model:

- The drag and lift coefficients, C_D and C_L, as functions of the ratio of rotational speed to stream speed and Reynolds number should be obtained from the experimental data. Like the Figure 18 in Sec. 3.1.

- The asymmetry of carry and time for a golf ball may need to be considered.

- The bouncing and rolling of a golf ball after touching the ground may need to be considered.

- ...

Also, the interaction between the clubhead and golf ball may need to be considered more. It maybe not just follow the simple equation like Eq. 30 in Sec. 2.5.

References

[1] L. D. Landau, E. M. Lifshitz, *Mechanics*, 3rd Edition, Elsevier, New York, 1976.

[2] Theodore P. Jorgensen, *The Physics of Golf*, 2nd Edition, Springer, New York, 1999.

[3] David M. Bourg and Bryan Bywalec, *Physics for Game Developers*, 2nd Edition, O'Reilly, 2015.

[4] Maxima, a Computer Algebra System, http://maxima.sourceforge.net/.

[5] Body Segment Data: http://www.exrx.net/Kinesiology/Segments.html.

[6] John Wesson, *The Science of Golf*, Oxford, New York, 2009.

[7] Katsumi Aoki, Koji Muto and Hiroo Okanaga, *Aerodynamic Characteristics and Flow Pattern of a Golf Ball with Rotation*, 8th Conference of the International Sports Engineering Association (ISEA), $2431 - 2436$, Procedia Engineering 2 (2010).

[8] A. Kharlamov, Z. Chara and P. Vlasak, *Magnus and Drag Forces Acting on Golf Ball*, Colloquium Fluid Dynamics, Institute of Hydrodynamics AS CR, v.v.i., Prague, October $24 - 26$ (2007).

[9] A Raymond Penner, *The Physics of Golf*, Rep. Prog. Phys. **66**, $131 - 171$ (2003).

[10] The Basic Python package, https://www.python.org/.

[11] The Numerical Python package, http://www.numpy.org/.

[12] The Python Plot package, http://matplotlib.org/.